X-HALE: THE DEVELOPMENT OF A RESEARCH PLATFORM FOR THE VALIDATION OF NONLINEAR AEROELASTIC CODES

THESIS

Alexander A Kaszynski, 2nd Lieutenant, USAF

AFIT/GAE/ENY/11-M15

DEPARTMENT OF THE AIR FORCE
AIR UNIVERSITY

AIR FORCE INSTITUTE OF TECHNOLOGY

Wright-Patterson Air Force Base, Ohio

AFIT/GAE/ENY/11-M15

X-HALE: THE DEVELOPMENT OF A RESEARCH PLATFORM FOR THE VALIDATION OF NONLINEAR AEROELASTIC CODES

THESIS

Presented to the Faculty

Department of Aeronautics and Astronautics

Graduate School of Engineering and Management

Air Force Institute of Technology

Air University

Air Education and Training Command

In Partial Fulfillment of the Requirements for the

Degree of Master of Science in Aeronautical Engineering

Alexander A Kaszynski

2nd Lieutenant, USAF

March 2011

AFIT/GAE/ENY/11-M15

X-HALE: THE DEVELOPMENT OF A RESEARCH PLATFORM FOR THE VALIDATION OF NONLINEAR AEROELASTIC CODES

Alexander A Kaszynski

2nd Lieutenant, USAF

March 2011

Approved:

Lt Col Christopher M. Shearer, USAF (Chairman)	date
Dr. Eric D. Swenson, Ph.D (Member)	date
Dr. Donald Kunz, Ph.D (Member)	date

Abstract

In conjunction with the Air Force Institute of Technology (AFIT) and the Air Force Research Laboratory (AFRL), the University of Michigan has designed and is currently building a remotely piloted aircraft (RPA) experimental high altitude long endurance (X-HALE) aircraft from which non-linear aeroelastic data will be collected to validate HALE aircraft design codes developed by academia, industry, and the federal government. While X-HALE is representative of HALE aircraft, the manufacturing and evaluation techniques are applicable to larger full size HALE aircraft such as the concepts being developed under Defense Advanced Research Projects Agencys (DARPA's) Vulture program. This thesis documents the development of the X-HALE model to date including a history of the programmatic decisions, basic model configuration, geometric considerations, sensor and system architecture, and manufacturing challenges. Lessons learned from the prototyping include the evolutionary growth of X-HALE's joiner blocks and the manufacturing process of the composite wings. Furthermore, late in the design process, a series of aeroelastic simulations using the Nonlinear Aeroelastic Simulation Toolbox (NAST) developed at the University of Michigan demonstrated the need for a rotating vertical/horizontal stabilizer to aid in the recovery of the vehicle from unstable nonlinear coupled lateral dynamic "dutch roll like" motion. The documentation and development of X-HALE is critical to the program's goal of providing a complete nonlinear aeroelastic data set for the validation of nonlinear aeroelastic analytical tools for government, industry, and academia.

Acknowledgements

First and foremost, to my wife: You've been there every step along the way with your loving support. Besides caring for our son and helping me dust the cobwebs from the cellars of my brain, I have her to thank for my faith in myself and in God.

To my brother: It is strange that one only feels the lack of companionship when one is without it. I will surely miss our time together as we now move in our separate Air Force directions, but I will never forget the time and adventures I have been lucky enough to have with you.

Finally, to my parents: If my son is any indication of how I was as a child, I now understand why you've said, "Just wait until you have kids." Thank you for bringing me up in a loving household and helping me set my path in life.

Alexander A Kaszynski

Table of Contents

List of Figures

Page

List of Tables

Page

List of Abbreviations

Abbreviation	
AAW	Active Aeroelastic Wing
AFIT	Air Force Institute of Technology
AFRL/RB	Air Force Research Laboratory Air Vehicles Directorate
ATV	Aeroelastic Test Vehicle
BWB	Blended Wing Body
CFD	Computational Fluid Dynamics
CG	Center of Gravity
CNC	Computer Numerical Control
COTS	Commercial off the Shelf
DARPA	Defense Advanced Research Projects Agency
DOD	Department of Defense / Depth of Discharge
EOM	Equations of Motion
ESC	Electronic Speed Controller
FTV	Flight Test Vehicle
GPS/INS	Global Positioning System / Inertial Navigation System
GPSr	Global Positioning System Receiver
HALE	High Altitude Long Endurance
HiLDA	High Lift over Drag Active Wing
ICE	Internal Combustion Engine
ISR	Intelligence, Surveillance and Reconnaissance
I/O	Input/Output
LCO	Limit Cycle Oscillation
NATASHA	Nonlinear Aeroelastic Trim and Stability of HALE Aircraft
ONERA	Office National d'Etudes et de Recherches Aérospatiales
PPS	Pulse Per Second
RCAS	Rotocraft Comprehensive Analysis System
RPA	Remotely Piloted Aircraft
RPM	Rotations Per Minute
SBC	Single Board Computer

UM/NAST	University of Michigan’s Nonlinear Aeroelastic Simulation Toolbox
UM/VABS	University of Michigan’s Variation Analytic Beam Solver
X-HALE	Experimental High Altitude Long Endurance

X-HALE: THE DEVELOPMENT OF A RESEARCH PLATFORM FOR THE VALIDATION OF NONLINEAR AEROELASTIC CODES

I. Introduction

In the past decade, the Department of Defense (DOD) has seen dramatic increases for sustained aerial reconnaissance and high altitude atmospheric research. Due to the limits of human endurance, Remotely Piloted Aircraft (RPA) are an excellent resource for maintaining a constant aerial presence in an operations theater [39]. While current RPA platforms have proved valuable, advances in airborne sensors and other real world constraints have driven airborne surveillance to higher altitudes not attainable by existing airframes. High Altitude Long Endurance (HALE) aircraft are the next generation of Intelligence, Surveillance, and Reconnaissance (ISR) platforms. In order to optimize their endurance, HALE aircraft are required to have a fuel fraction greater than 66%, which leads to these sensorcraft having very small structural weight fractions as well as highly efficient and aerodynamic bodies [36]. The aircraft's high aspect ratio and low structural reinforcement leads to a vehicle that operates and performs differently than its rigid body counterpart. These HALE aircraft tend to have low wing loading compared with their rigid body counterparts. Furthermore, large deformations in HALE aircraft, both statically and dynamically, require a different analysis of flight dynamics compared to more rigid aircraft. New methods of analysis are needed to help in the development of new control models so that effective HALE RPA controllers can be developed. Additionally, due to the high wing deformations as well as low frequency natural structural vibration modes, HALE aircraft must be designed so that they are inherently stable and have controllers that incorporate known bounds of stability.

The limitations of traditional controllers and linear structural analysis were highlighted during the Helios (Figure 1) incident, a precursor to the Defense Advanced Research Projects Agency (DARPA) Vulture program.

Figure 1. Aerovironment's Helios

During a routine flight test on 26 June 2003 near the Navy Pacific Missile Range Facility on the island of Kauai, Hawaii, the Helios aircraft encountered turbulence causing the wings to morph into an unexpected, persistent, high dihedral configuration. Due to the high dihedral, the aircraft developed a divergent pitch mode which lead Helios to exceed its maximum design airspeed. The resulting high dynamic pressures caused the solar panels on the upper surface of the wing to separate and the resulting structural damage to the wing led Helios to lose the ability to remain airborne. Helios impacted the surface of the ocean and was destroyed [17]. It was determined that the root cause of the mishap was the preflight analysis which was based on linear structural analysis software

that did not accurately estimate the effects of disturbances on this very flexible body. The strongest recommendation from the report regarding the failure of Helios was to develop more advanced multidisciplinary time-domain analysis to approximate highly flexible aircraft.

In parallel to this recommendation, Eric Brown, Chris Shearer, and Weihua Su with guidance from Carlos Cesnik have developed an analytical solution to the coupled nonlinear aeroelasticity and flight dynamics of very flexible aircraft [27]. The University of Michigan's Nonlinear Aeroelastic Simulation Toolbox (UM/NAST) is the framework that seeks to accurately represent and analyze HALE or very flexible aircraft such as Helios. On 27 August 2008, Shearer, Appendix 1, proposed to the University of Michigan's Solar Bubbles team that an adaptable aircraft be created in order to validate nonlinear solvers such as the Rotocraft Comprehensive Analysis System (RCAS), ASWING, Nonlinear Aeroelastic Trim and Stability of HALE Aircraft (NATASHA), and UM/NAST. On 10-11 September 2008 there was a DARPA Vulture sponsored meeting on nonlinear aeroelasticity. During that meeting it was confirmed that there was no comprehensive set of data of an aircraft flight test and as built information that could be used to validate nonlinear aeroelastic codes [30]. Representatives from AFIT, AFRL, and the University of Michigan decided to build a low-cost free-flying test bed for nonlinear aeroelastic code validation. While Shearer gave inputs and suggestions, X-HALE was developed and designed by the University of Michigan and was sponsored by the Air Force Research Laboratory Air Vehicles Directorate (AFRL/RB). This aircraft, currently under production, will gather aerodynamic and aeroelastic data during flight tests. The research effort contained in this thesis seeks to organize and analyze the

current ongoing construction of X-HALE. This effort seeks to inform and to aid the construction efforts of larger scale aircraft, to include DARPA's Vulture program.

II. Theoretical Development

2.1 Previous research and Motivation

Since X-HALE is designed to validate nonlinear aeroelastic solvers, a brief history, the development, and the uses of several codes follow. The bulk of research into the problem of nonlinear aeroelasticity coupled with nonlinear flight dynamics began in the 1990's with van Schoor and von Flotow. Their work determined that when analyzing non-rigid aircraft, the aircraft structural dynamics must be taken into account This is mainly due to the feedback that results from the changing flight structure that changes the aircraft's modes in all three axes [38]. Patil, Hodges and Cesnik studied the aeroelastic dynamics of HALE aircraft, which is of critical importance considering that highly flexible aircraft are much more likely than standard aircraft to produce aeroelastic phenomena such as flutter and buffeting. A significant discovery of the research team was that a linear aeroelastic analysis does not correctly represent the natural modes of a very flexible aircraft [19]. As a result, it is possible for a linear aeroelastic analysis to ignore the shifting of a wing's natural mode that may cause the wing's flutter velocity to fall to aircraft's cruise velocity. Continuing the research, Patil, Hodges, and Cesnik discovered the erratic behavior that can develop from large deflections of flexible wings. It was found that self-reinforcing interactions between the wing structure and the normal loads fed into the same behavior that would have most likely predicted the Helios incident. Additionally, it was discovered that the short period and phugoid modes obtained using standard linear aeroelastic techniques are significantly different than with using those obtained by non-linear aeroelastic techniques.

Parallel to Cesnik's research efforts, Drela has created another tool for analyzing the aerodynamic, structural, and control-law design of a very flexible aircraft. ASWING, a nonlinear aeroelastic code, provides the ability for the designer to rapidly analyze the aircraft during the early phases of aircraft development [7]. It utilizes a geometrically nonlinear isotropic beam analysis and lifting line aerodynamics coupled with a one-lag term for unsteadiness corrections. Patil and Hodges also developed NATASHA [18]. This computer code was based upon previous theoretical work where the governing equations were the geometrically-exact equations of motion that were written in their intrinsic form and augmented with intrinsic kinematical equations [12]. It has been utilized for joined wing aircraft through the use of an incremental method to find a trim solution and the fully intrinsic equations to perform eigenvalue analysis about the steady-state solution [20].

Furthermore, the Rotorcraft Comprehensive Analysis System (RCAS) is used for modeling complex rotorcraft configurations in various maneuvering conditions. The RCAS code uses a finite-element, multibody-dynamics formulation for coupled rotor-body systems and can be applied to HALE aircraft due to its high fidelity in coupled solutions. The system uses an input data processer, structural and aerodynamic models, and numerical solution utilities. Several aerospace corporations have utilized RCAS for structural dynamic analysis due to the fact that RCAS uses exact element formations that enable the analysis of a full range of steady and maneuvering flight conditions [22].

Jones conducted research into the design of HALE vehicles and concluded that standard aircraft design techniques do not apply to these aircraft [15]. This is mainly due to the fact that HALE vehicles by necessity must have high-aspect-ratio wings as well as

a significant proportion of their mass allocated to fuel rather than structure. As a result, these aircraft tend to be highly flexible and subject to aeroelastic phenomena to include flutter.

The bulk of the aeroelastic analysis of X-HALE was performed by UM/NAST. The University of Michigan's Nonlinear Aeroelastic Simulation Toolbox was first developed by Brown by the guidance of Cesnik at MIT and then continued at the University of Michigan under Shearer and Su under the direction of Cesnik. Built using Matlab, the framework analyzes composite beam structures to determine wing bending modes, wing deflections due to static and dynamic loading, stresses, and strains. Brown originally wrote the code and developed the basic formulation. This code was further developed by Shearer in 2006 where he improved upon the governing differential equations and numerical integration [27]. Shearer refined the governing flexible and rigid body equations of motion (EOM) and introduced a stable long term numerical integration framework. Additionally, he began the development of basic control laws for HALE aircraft. Su incorporated nonlinear buckling, algebraic constraints, and performed several analyses on joined, flying wings, and structural nonlinearities [34].

The code was modified to include three types of time simulations: rigid body, linearized, and nonlinear. The aeroelastic solver models slender, flexible aircraft as beams. Structural coupling between joined members are modeled through nodal displacement constraints. After the aircraft model is initialized, the code determines the natural modes and frequencies of the structural system. The solver then returns the static deformation based upon flight loading. The solver then iterates until it converges on a

nonlinear static deformation. The code can also solve the time marching problem by assuming a rigid, linear, or nonlinear analysis.

Additional research that utilized UM/NAST included the analysis of the nonlinear aeroelasticity of a flapping wing Micro Air Vehicle (MAV) [33]. The nonlinear aeroelastic solver incorporated two unsteady aerodynamic formulations and the researchers were able to conclude that the finite-state inflow theory was suitable for flapping wing simulations.

2.2 Past Wind Tunnel Testing of Highly Flexible Wings and Future HALE Applications

It is important to discuss previous research regarding real time testing of flexible wing structures in order to validate the research importance of X-HALE. Jaworski conducted wind tunnel testing on an accelerometer equipped wing by cycling the tunnel's wind speed beyond the wing's flutter point and then reducing the speed until the static state was recovered [14]. The testing measured the speed, limit cycle oscillation (LCO) amplitude, and hysteresis of the wing's flutter. The wing was modeled using the slender body assumption by representing the beam using simplified Hodges-Dowell equations and aerodynamically using classical Theodorsen thin airfoil theory and the ONERA dynamic stall model. Developed in the 1980's, the Office National d'Etudes et de Recherches Aérospatiales (ONDEA) determines the two-dimensional aerodynamic forces on an airfoil using a semi-empirical unsteady, non-linear model. This experiment found that the slender body assumption and ONERA dynamic stall models accurately predicted the flutter speed and aeroelastic phenomena. It was also found that the nonlinear elastic coupling was the key feature necessary to model the limited cycle oscillations and flutter

frequency. This experiment helps to validate some of the modeling used in UM/NAST, but since it does not simulate the aeroelastic phenomena of a free flying HALE wing, it cannot be used to validate the code in its entirety.

The Active Aeroelastic Wing (AAW) program conducted wind tunnel testing on a scaled down model of a production F/A-18A with an Active Flexible Wing [8]. The AAW program investigated the potential benefits a flexible wing would provide, specifically in the transonic flight regime. The program identified and evaluated several issues to include matching the dynamic aeroelastic properties of the full scale model with the model [10]. Once the data from the wind tunnel testing had been reduced and analyzed, the program proceeded to incorporate the lessons learned into a full scale model and continued testing and deforming the thin swept wings for optimum aerodynamic performance. This research promoted the use of a scaled model to represent the aeroelastic behavior of a full scale aircraft. While X-HALE does not seek to represent any specific full scale HALE aircraft, X-HALE does seek to duplicate the same aeroelastic phenomena present in full scale HALE aircraft in order to validate nonlinear aeroelastic solvers.

Tang and Dowell have also conducted wind tunnel testing similar to Jaworski's work. Using the same nonlinear beam theory assumptions in combination with empirical ONERA aerodynamic stall data, Tang and Dowell studied the effects of geometric structural nonlinearity on the limit cycle oscillations of a high aspect ratio wing. The experimental data obtained from the wind tunnel were in agreement with the theoretical flutter expectations based on the aforementioned model. Like Jaworski's work, this experimentation helps to verify the framework used for the nonlinear aeroelastic solves,

but fails to validate a full aircraft model. UM/NAST models aircraft using multiple beam structures and additional testing is necessary to validate a multiple node model.

2.3 Aeroelastic Tailoring

X-HALE's wings are aeroelastically tailored to use lightweight and flexible materials to create a strong and predictable wing structure, yet flexible enough to excite structural modes that are within the same order of magnitude as the rigid body modes. While aeroelastic tailoring was not one of X-HALE's research goals, X-HALE did utilize aeroelastic tailoring through the use of the University of Michigan's Variation Analytic Beam Solver (UM/VABS). Aeroelastic tailoring is by no means a new technology. Shirk, Hertz, and Weisshar [31] conducted research into modifying the number and direction of plys in order to favorably affect the characteristics of the wing structure. In general, whenever the number of plies or the laminate direction is specifically modified or selected for a composite aircraft, the aircraft's design is said to being aeroelastically tailored. While tailoring may increase the complexity of the aircraft design and manufacturing, this is usually offset with the increased performance resulting from the modification. Since aeroelasticity is dependent on the interaction between the deformation of the lifting surface and the aerodynamic loads on that surface, by increasing or decreasing the stiffness of the wing in one or more directions, it is possible to increase the strength of the wing structure without drastically increasing the mass of the wing or adversely increasing the stiffness.

2.4 Requirements for the Low Cost Experimental HALE Test Bed

The experimental HALE test vehicle must be able to collect data from flight testing consisting of a series of tests stimulating gust and roll perturbations. Furthermore,

this aircraft must also share similar characteristics to a HALE aircraft. These characteristics include: 1) A high aspect ratio, 2) Low wing loading, 3) High static wingtip deflections (greater than 10%), and low frequency structural modes. Due to the endurance required of HALE vehicles, these aircraft must operate at high altitudes at low power, thus requiring a high aspect ratio. This is because the main driver for reducing the drag while holding wing area constant is increasing the aspect ratio. The drag term effected by the aspect ratio is the coefficient of induced drag given in Equation 1 below.

$$\frac{\qquad}{\qquad} \tag{1}$$

Increasing the aspect ratio not only lowers the induced drag, but also increases the Oswald efficiency factor (e). A high aspect ratio decreases the induced drag of an aircraft and increases its lift-to-drag ratio allowing its on-station time to be maximized. The aspect ratio must be relative large, generally on the order of 30 to 40 to achieve the drag reduction benefits before structural constraints prevent an increase in aspect ratio. A HALE test vehicle's aspect ratio should reflect that of a full scale HALE vehicle in order to properly demonstrate the aeroelastic phenomena and bending stresses associated with the long and flexible wings. Table 1 lists the aspect ratios of selected HALE aircraft.

Table 1. Aspect Ratios of Selected HALE Aircraft

Aircraft	Aspect Ratio
U-2	10.6
Helios (NASA Pathfinder)	31
Qinetiq Zephyr	22
DARPA's Vulture	40
Solar Impulse	19.7
White Knight	20

Of the listed HALE aircraft, with the exception of the U-2, all have aspect ratios greater than 19.7. Aeroelastic phenomena, while present even in wing structures with low aspect ratios, become more pronounced in wings with high aspect ratios. While X-HALE seeks to collect data for code validation, it is important to recognize that it should mimic the aeroelastic properties of similar HALE aircraft. With an aspect ratio of 30 or 40, depending on the modular wing configuration, X-HALE's aspect ratio would match NASA's Helios's and DARPA's Vulture. Figures 1 through 6 show the aircraft listed in Table 1.

Figure 2. U-2 [37]

Figure 3. DARPA's Vulture [3]

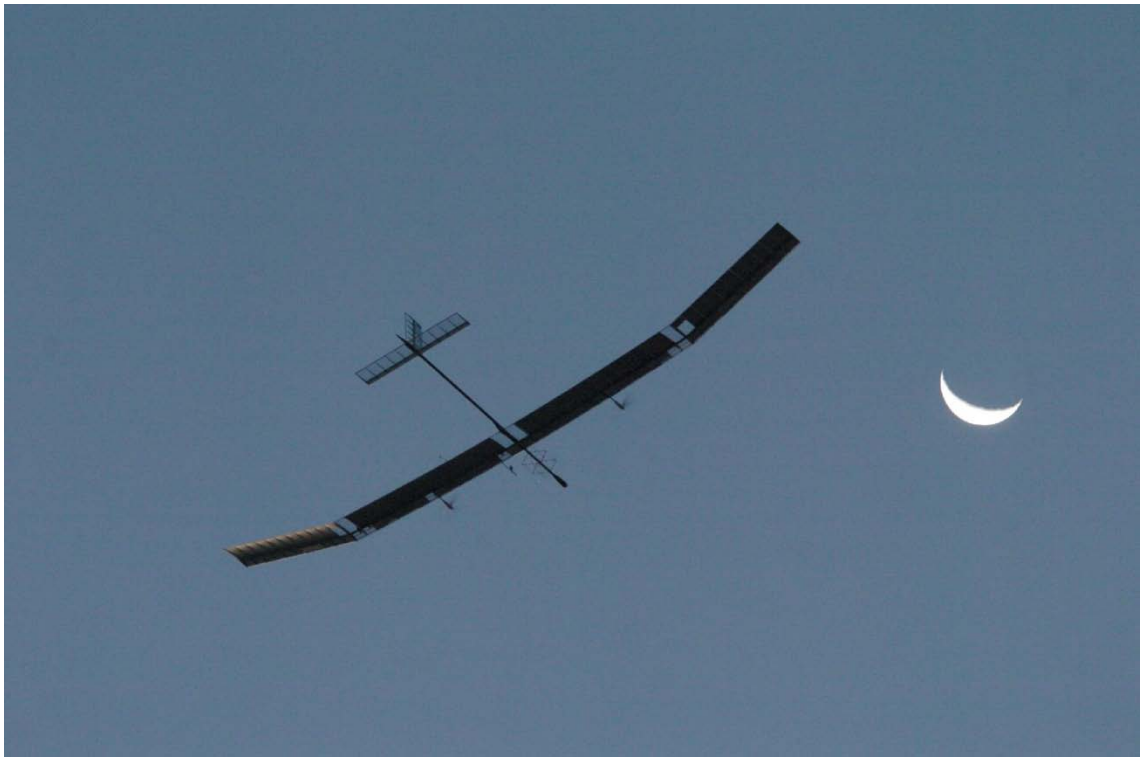

Figure 4. Qinetiq Zephyr [8]

Figure 5. Solar Impulse [2]


Figure 6. White Knight [9]

In order to stress the nonlinear aeroelastic effects that result from the aircraft's flight dynamics and the aircraft's structure, the HALE test vehicle should exhibit high wingtip deflections. With wingtip deflections greater than 10%, linear elastic theory begins to break down and higher-order nonlinear terms must be included. The HALE aircraft must utilize the correct materials and manufacturing techniques in order to guarantee that the aircraft does not fail structurally during flight while still maintaining the flexibility required for at least a 10% deflection. Additionally, the test HALE aircraft must also be able to initiate and recover from longitudinal and lateral instabilities via manual and automatic control.

In order to validate the code for nonlinear aeroelastic solvers, the test HALE aircraft must also be able to acquire real-time flight test data. This sensor data should include at a minimum the commanded input to all control surfaces; lateral, longitudinal, and vertical axis positions and velocities; airspeed at multiple locations; and three axis strains throughout the wings. Housekeeping data to include battery voltage and current if electric, the engine RPMs, or temperature sensors for both electric and internal combustion engine (ICE) configurations would be necessary for initial aircraft testing, but are unnecessary for code validation. The aircraft should have radio controller inputs for manual control as well as an onboard digital controller in order to facilitate the development of an automatic control system for code verification and closed-loop controller development and validation. This controller should be able to be manually overridden to avoid aircraft damage in the case of a faulty control module.

Optimally, the HALE test aircraft would be 1:1 to past representative HALE aircraft. However this would require funding beyond the scope of X-HALE. AFRL/RB

would be unable to fund such a project when a more economical aircraft could validate the nonlinear aeroelastic codes mentioned in the previous sections. Additional factors to consider are the manpower and time constraints students at the University of Michigan have in regards to building the test aircraft. Therefore, the size should be reasonably limited in order to limit costs. Provided the aspect ratio, wing deflection, and bending modes are within the proper specifications, the aircraft's size should not matter for initial code validation purposes. In order to increase the ease of transport of the test aircraft, the aircraft should be small enough to be easily transportable either by disassembly or transport of the entire assembled aircraft.

Due to Federal Aviation Administration (FAA) limitations, remotely piloted vehicles cannot be operated within controlled airspace or above 400 feet above ground level. While this aircraft is effectively a radio controlled aircraft, it does not meet the FAA's regulations for R/C aircraft. Therefore, in order for it to be operated under the new FAA regulations, it must be flown under a Certificate of Authorization (COA) or within a restricted airspace. Without a COA being certified by the FAA, the HALE test aircraft cannot be tested at Wright Patterson Air Force Base (WPAFB) or at the University of Michigan. This increases the need for a highly transportable aircraft in order to transport it to a military restricted area so that it can be flown without a COA.

III. How the Requirements Evolved into X-HALE

3.1 Initial Design Parameters

Stemming from Shearer's initial presentation [26] and in response to the September 2008 DARPA meeting, the University of Michigan created an initial design based upon the requirements in Section 2.4. The following chapter details the design analysis and material selection process.

The research data acquisition aircraft's initial design recommendations came from Shearer's presentation on 27 Aug 2008 [26], Appendix A-1. Shearer recommended that the wing span be approximately 3 meters, the aircraft have multiple wing sets to include a rigid set (0-5% tip deflection), a linear set (less than 10% tip deflection), and a nonlinear set (30% or greater tip deflection). The aircraft would have the ability to drop weight in flight in order to simulate fuel loss. Shearer also recommended that the aircraft be able to measure wing displacement or strain, angular accelerations and velocities, and would be able to determine its inertial position and orientation. This data would have to be stored, either onboard via data storage, or transmitted in real time off board to a data storage receiver. Finally, the recommended aircraft should remain airborne for 45 minutes and would have programmable surface deflections (to include step inputs, sinusoidal sweeps, etc.).

Shortly after the September 2008 DARPA Nonlinear Controls meeting Carlos Cesnik, Patrick Senatore, and to a lesser degree, Christopher Shearer took part in beginning the initial design process for the data acquisition aircraft. The research team chose the name X-HALE (Experimental HALE) for the aircraft and it was originally planned to fly in the fall of 2009.

3.2 Aircraft Configuration and Initial Design Considerations

Due to the predicted cost of the aircraft's sensors and the necessity of prototype testing, it was decided that two models of X-HALE would be created. Using inter-compatible parts, the X-HALE program would have a flight test vehicle (FTV) and an aeroelastic test vehicle (ATV). The FTV would only include housekeeping sensors and a minor set of aeroelastic sensors to record the health of the aircraft. X-HALE's initial properties were inspired from a HiLDA (High Lift over Drag Active Wing) wind-tunnel model [6]. See Figure 7 below.

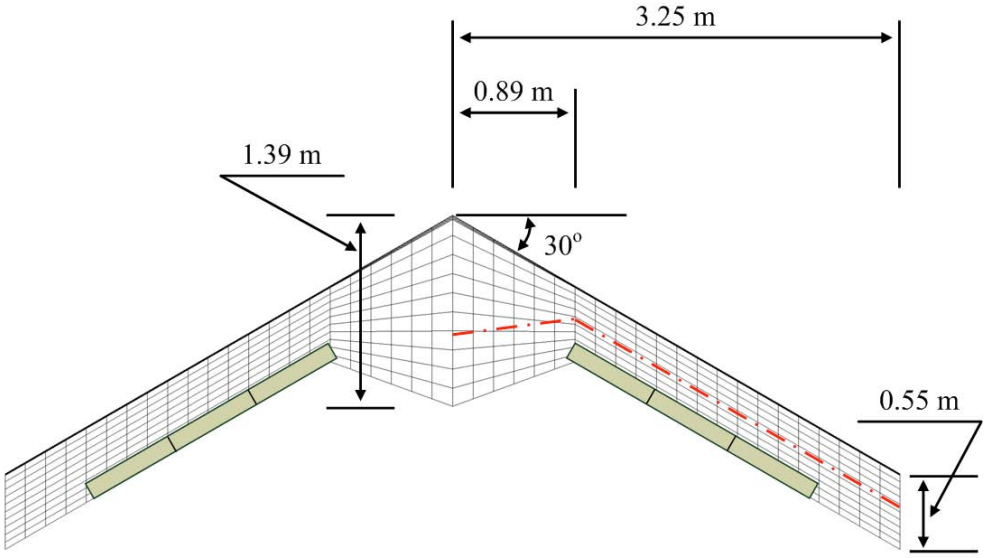

Figure 7. HiLDA Wind-Tunnel Model [5]

In order to simplify the design process and the computational model used for nonlinear code validation, X-HALE's designers chose to avoid the blended wing body (BWB) configuration and incorporate only the flying wing concept. To give the reader a better expectation of the overall design of X-HALE, a generic model will be introduced and modified during sections of this chapter where the model is modified. The initial design, based mostly upon the expectations of Shearer's presentation, can be found below

in Figure 8. The initial design assumed a single high dihedral flying wing with control surfaces incorporated into the wing.

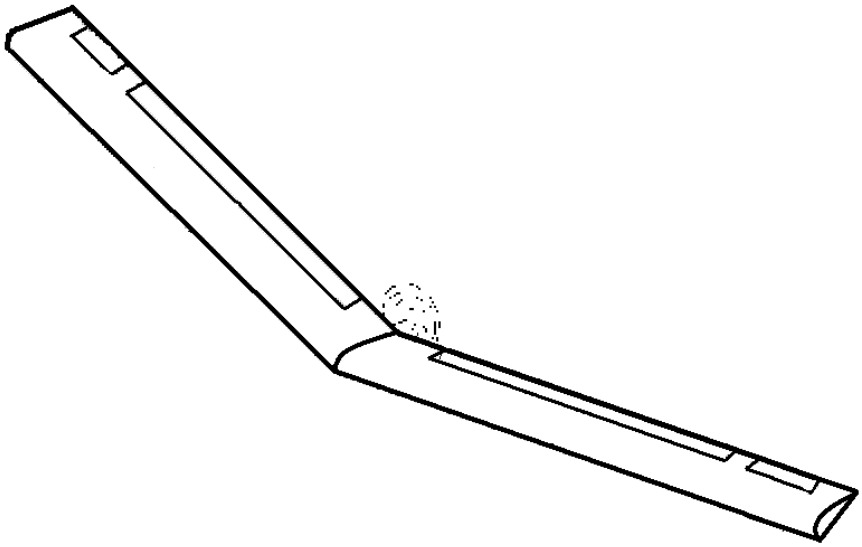

Figure 8. Preliminary X-HALE Design

3.3 Wing Design Considerations

The driving factor for the creation of X-HALE was the ability for the aircraft to provide nonlinear aeroelastic data during flight testing. Therefore, wing design included some of the most critical design choices. For the data from X-HALE's flight testing to be valuable for nonlinear aeroelastic solvers, X-HALE's wings had to have a high aspect ratio, low wing loading, and greater than 10% wing tip deflection.

A joined wing was never considered because of the local stiffness and nonlinearities introduced at the joints and since joined wings are usually only considered when a large area for sensors is needed. The simplicity of a flying wing makes it stand out as a reasonable choice considering that a joined wing aircraft must take into account stresses at joint mechanisms and the effects of those joints on the structure of the aircraft. It was decided that X-HALE would use a flying wing configuration in order to simplify the

aircraft and to ensure that the aircraft would remain flexible enough to generate the data required for code validation.

If the wing was to be manufactured using composite materials, the University of Michigan's autoclave limited the size of the wing to approximately one meter. Since the key features of HALE aircraft include the intermixing of structural and rigid body modes and a high aspect ratio, a one meter wing would have a very small chord. Thus, it was decided that X-HALE would incorporate modular construction of its wings. This was done in order to ensure that the aircraft was large enough to be able to imbed sensors, actuators, and other hardware within the wings and in the fuselage while producing a 1st structural mode of less than 1 Hz. It was decided that the two outer wing sections would have a 10° angle in order to increase the lateral stability of the aircraft. See Figure 9 below for the preliminary X-HALE design with the flying wing incorporated. This figure does not include propulsion or a fuselage and is not to scale.

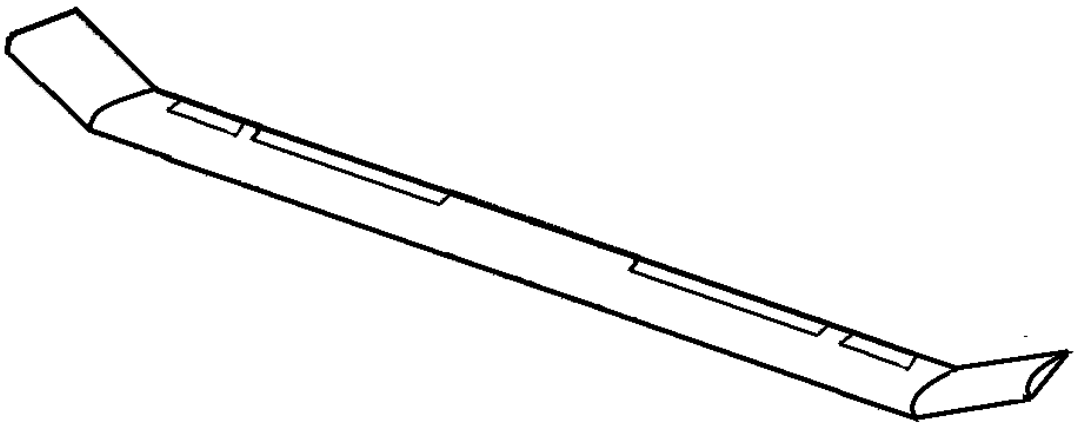

Figure 9. Preliminary X-HALE with Incorporated Flying Wing Design

For the purpose of the UM/NAST code validation, it was decided that the wing should consist of a load carrying beam approximately centered on the quarter chord of the

airfoil with the rest of the airfoil left empty of load bearing structures. This design choice was made due to the fact that UM/NAST represents structural members as beam elements. Sensor data from X-HALE would be able to best validate nonlinear aeroelastic codes if the aircraft matched the models used for those codes. A reflexed airfoil was selected due to its applicability to an all flying wing. Given an increased angle of attack, due to a gust or control input, conventional airfoils will have a tail heavy moment since the lift is larger than the moment at the quarter chord. Conventional airfoils would pitch up when disturbed with a positive angle of attack. Aircraft with a conventional airfoil require a tail with a horizontal stabilizer to combat the negative pitch moment induced by the airfoil. Airfoils with a reflexed mean chord line will pitch down when disturbed with a positive angle of attack. An aircraft using a reflexed wing would not require additional control surfaces and would minimize the complexity of the aircraft. Figure 10 below shows a sample reflexed airfoil.

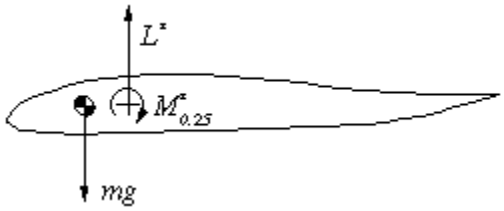

Figure 10. Reflexed Airfoil [11]

3.4 Wing Material Considerations

Initially, X-HALE's designers considered building the wing out of a single large piece of aluminum. However, since the nonlinear aeroelastic solvers, to include RCAS, NATASHA, and ASWING all use a beam element to model the wing, it would be unreasonable to expect accurate data from a wing with multiple spars and ribs. In order to build the wing as close as possible to a single beam the design would have to

incorporate a “wing box.” The wing box is effectively a central beam that carries the structural and aerodynamic loads and is centered at quarter chord of the wing. While it may have been possible to use aluminum as the primary construction material, it was much easier to aeroelastically tailor a composite wing rather than a metallic wing. Using the UM/VABS, it was possible to aeroelastically tailor the flexibility of the wing by selecting the type of composite material and the number and the direction of the plys. This would give the design team control over the stiffness and strength of the wing.

Four mainstream composites were considered for the wing: carbon fiber, E-Glass, S-Glass, and aramids (Kevlar). Boron-fibers were not considered due to the difficulty of construction and high stiffness. Table 2 shows the relative strengths and characteristics of popular composites. Figure 11 below the relative costs of those composites.

Table 2. Summary of Composite Characteristics [1]

		Glass fiber composites				Carbon fiber composites				
	Units	E	S	Boron	Aramid K 49	HT	HM	UHM	Al	Ti
SG	—	2.1	2.0	2.0	1.38	1.58	1.64	1.7	2.76	4.4
α_1	μm/°C	7.1	6.3	4.5	−1	−0.16	—	—	23	9
α_2	μm/°C	20	—	—	70	24	—	—	23	9
σ_{1tu}	MPa	1020	1620	1520	1240	1240	760	620	454	1102
σ_{1cu}	MPa	620	690	2930	275	1100	690	620	280*	1030*
σ_{2tu}	MPa	40	40	70	30	41	28	21	441	1102
τ_u	MPa	70	80	90	60	80	70	60	275	640
ILS	MPa	70	80	90	60	80	70	60	—	—
E_1	GPa	45	55	210	76	145	220	290	72	110
E_2	GPa	12	16	19	5.5	10	6.9	6.2	72	110
G_{12}	GPa	5.5	7.6	4.8	2.1	4.8	4.8	4.8	27	41
ν_{12}	—	0.28	0.28	0.25	0.34	0.25	0.25	0.25	0.33	0.31
ε_{1u}	—	0.022	0.029	0.006	0.016	0.01	0.03	0.02	0.12	0.06
ε_{2u}	—	0.4	0.4	0.4	0.5	0.4	0.4	0.3	—	—

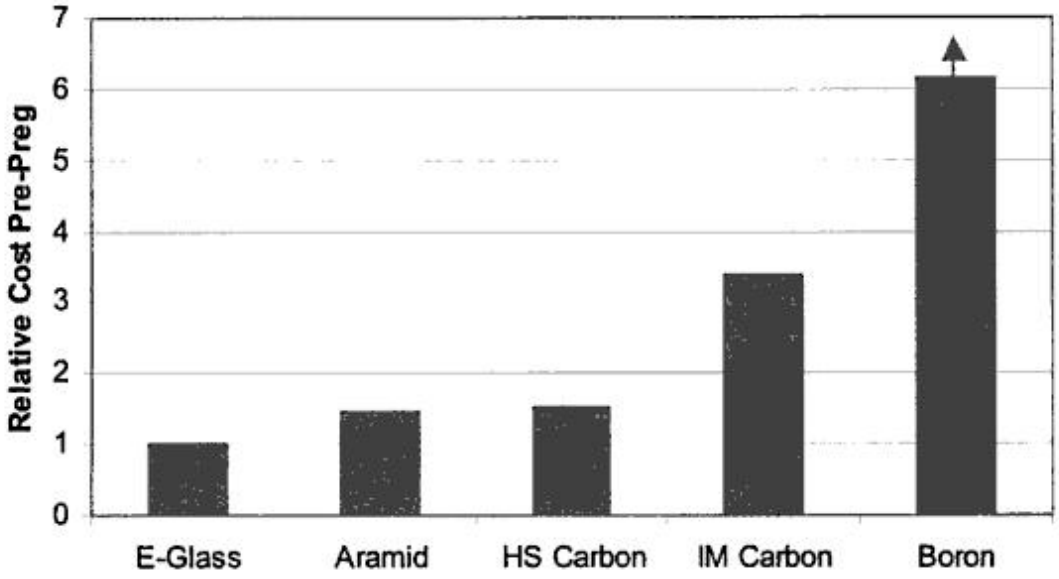

Figure 11. Relative costs of Selected Pre-Preg Composites [1]

E-Glass, used extensively in gliders, has the major advantage of relatively low cost and high strength. While carbon fibers have a much lower specific gravity and higher strength, carbon fibers are far too stiff to be applicable to X-HALE's wing, even considering UM/VABS. The low Young's Modulus of E and S Glass also increases their desirability as a skin choice for X-HALE due to their flexibility [1]. While Kevlar (aramid fiber) has a higher specific tensile strength, it also has the severe disadvantage of low compression resistance. Flexural loading present during the flight of X-HALE would likely cause non-linear plastic deformation by the formation of kink bands due to the extended chain structure of the aramid fibers. Therefore, Kevlar tends to be unstable under compression loading [1]. While this nonlinear behavior can be modeled within the NAST framework, additional unnecessary modeling is necessary and undesirable for initial code validation. Therefore, Kevlar would not be used for X-HALE's wings. One drawback of using E/S glass composites is their high rate of fatigue. However, considering the limited endurance and short lifespan X-HALE and its flights, E/S-Glass

remains an optimal design choice due to its cost, strength, and flexibility. Of the two, E-Glass was selected due to its lower cost than S-Glass.

3.5 Fuselage Design Considerations

To house sensors, data processing units, engines, and fuel, X-HALE would need a large fuselage to protect and streamline the components. In order to reduce point wing loading and the localization of mass, X-HALE would have distributed fuselages rather than one single large fuselage. These fuselages would be streamlined to reduce parasitic drag and would be mounted below the aircraft in order to provide surface contact for takeoff and landing. Using DARPA's Vulture and the Solar Impulse for inspiration, the fuselage modules would be incorporated into the flying wing according to Figure 12 below. The number of fuselage pods would be based on several factors to include: the number of motors required for flight, the number of sensors and data processing units required, and the number of ground contacts required so that the aircraft would not drag on the ground during takeoff and landing.

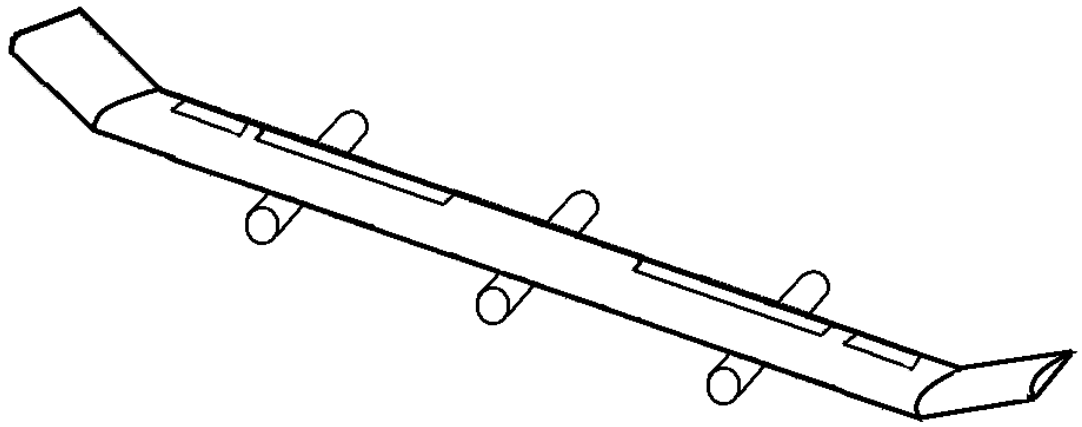

Figure 12. Preliminary X-HALE with Incorporated Fuselage Design

3.6 Propulsion Design Considerations

From the onset of the initial design process, the use of an ICE was not considered. While greater range and flight endurance could be gained through the use of ICE due to the energy density of carbon based fuels, the recommended duration according to Shearer was only 45 minutes [26]. Electric propulsion has the advantage of reduced operating costs, initial investment, low maintenance, simpler reparability, reliability, reduced fire hazard concerns, faster response times, and better controllability. For these reasons, X-HALE would use electric motors powered by onboard batteries. To reduce point loading and to utilize the multiple fuselage configuration, multiple motor and battery sets would be used. Not only would this distribute X-HALE's mass throughout the aircraft, but it would also permit the aircraft's controller to yaw X-HALE through differential thrust. The motors and batteries would be installed inside the fuselages. These motors would have to be powerful, yet efficient enough to ensure that X-HALE remains airborne for 45 minutes without requiring exceptionally large batteries.

3.7 Control Surface Design Considerations

The control surfaces for X-HALE would have to be large enough to allow the aircraft to take off, maneuver to remain inside the testing area, conduct flight testing, and to land. Following the flying wing concept, the control surfaces should resemble inboard elevons and outboard ailerons. However, due to the expected short airfoil chord to compensate for the combination of the high aspect ratio and small autoclave, it was not reasonable to incorporate large ailerons into the composite wings. The required hinges would unpredictably stiffen the wing, and the size of the wing would make the installation of ailerons far too complex. The choice was made to attach rear facing

booms to the fuselages in order to provide elevon control while minimally impacting the aeroelastic nature of the wings. While it would be possible to control X-HALE through the use of only one or two elevons, the designers wanted to ensure that there was sufficient control to excite the aircraft's structural modes. The number of control surfaces would have to be over designed. While the specific number of booms will depend on the mass properties of X-HALE, it is still possible to envision one tail boom attached to each fuselage as seen below in Figure 13.

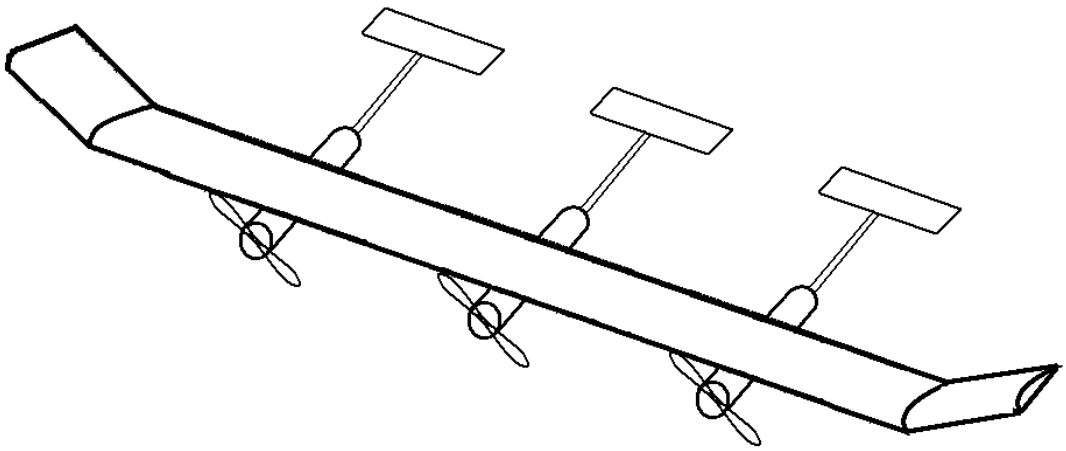

Figure 13. Preliminary X-HALE with Engine and Tail Booms Incorporated

3.8 Sensor Selection and Design Considerations

In order for X-HALE to meet the requirements as a data collection platform for the validation of several nonlinear aeroelastic codes, X-HALE must at a minimum include sensors to measure wing displacement or strain, angular accelerations relative to the body, and a way of determining the aircraft's inertial position and orientation. Since the nonlinear aeroelastic solvers track a body-fixed reference frame, knowledge of the linear and angular accelerations and velocities of the aircraft's only need to be limited to one

point on the aircraft, the origin of a body-fixed reference frame. Due to the flexibility of the aircraft, the origin may not necessarily be at the center of gravity (CG). Combining the sensors required to determine inertial position and orientation along with the angular accelerations and velocities would best reduce the aircraft's weight and cost. Data from a three-axis accelerometer could be integrated to ascertain velocities and positions at critical points during flight testing. However, the integrated positional data from even the most accurate accelerometers will drift even for a flight of a short duration of the suggested 45 minutes. Therefore, another sensor is required for determining the position and orientation of the aircraft. While quartz inertial sensors are available at a low cost, these sensors tend to exhibit relatively poor performance compared to conventional receivers and would lack the required fidelity for code validation. A gyroscope could provide the required accuracy regarding the inertial orientation of the aircraft. Only a relatively coarse estimate of the aircraft's position is required since positional data is not critical for code validation. A GPS would provide approximate positioning (commercially averaging ± 10 Meters) and velocity data that would verify the integrated accelerometer velocity data but would not be used specifically. Furthermore, a GPS would be able to provide pulse per second (PPS) timing that would synchronize data obtained from the aircraft's various sensors.

While the X-HALE will have two methods of measuring velocity, the presence of wind gusts and inaccuracies in the GPS or accelerometer require additional sensors to measure the aircraft's airspeed. Three five-hole pitot probes would measure airspeed by being mounted on each wing tip and near the center of the aircraft outside of prop wash. The five-hole pitot probes have the advantage over conventional pitot probes in being

able to indicate the velocity and direction of the relative wind. This type of pitot probe allows for more accurate computation of the aircraft's angle of attack, side slip angle, and actual air speed. This can be accomplished by measuring the differential pressures between the front most total pressure port and the adjacent ports as seen below in Figure 14.

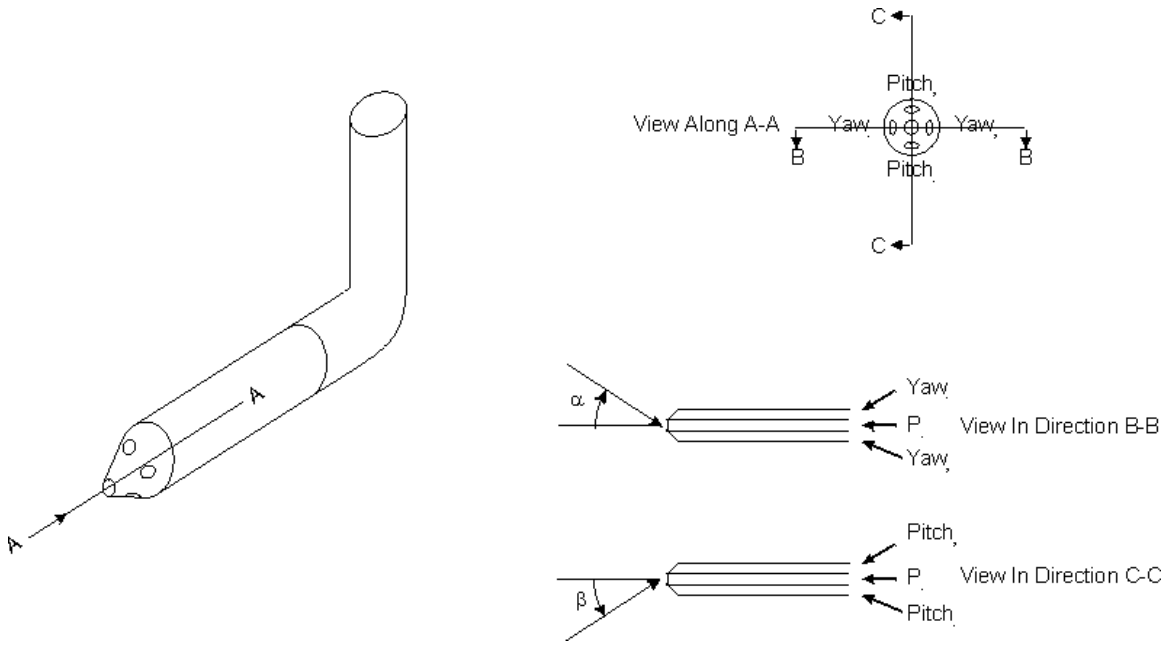

Figure 14. Sample Five Hole Pitot Probe [13]

In order to collect wing displacement data from the X-HALE, strain gauges must be placed throughout the wing. Since the wing boxes allow the wing to be represented as a beam, it is necessary for the strain gauges to be placed on the wing boxes themselves. It would be necessary to characterize the bending and torsional properties of the wing prior to flight, thus quantifying the relationship between the wing's strain and displacement. Strain gauges would be placed throughout the wing and would measure strain in the longitudinal and vertical directions as well as the torsion near the middle of the wing box.

Additionally, housekeeping sensors would be used for real time aircraft health reporting for ground crews controlling and monitoring X-HALE. Potentiometers placed on the tail would be used to measure the position of the elevons. Motor RPM sensors would report on the motors to the ground controllers to indicate if a motor failed or is not at the correct RPM. Thermocouples placed near the engine and temperature sensitive hardware would be used to track the temperatures of the aircraft's critical components and would allow ground controllers to power off aircraft components to avoid permanent damage.

3.9 Data Collection and Storage Design Configurations

Storing or transmitting the sensor data collected from X-HALE's sensors would require some sort of mobile computing platform. The platform would have to be able to interpret and digitally quantize data from the strain gauges, pitot probes, housekeeping sensors, and the inertial/GPS navigation system. Despite recent advances in computer miniaturization, a large computing platform will be required in order to process and store the data. Considering the modular fuselage design and the need to distribute fuselage loading throughout the aircraft, the design team determined the best choice for the computing platform would be to install a set of small, expandable, single board computers (SBC) throughout the aircraft to match the necessary sensor processing requirements. Measuring anywhere between 2" by 2" inches to 6" by 6", these small computers have the advantage of low power consumption, low weight, stackable modular expansion, and low heat generation. Since onboard power will have to be supplied by batteries, low power consumption is a key factor for choosing SBCs. Additionally, since these computers have the same capabilities as standard desktop computers, it will be

possible to link these computers together to a master SBC. This will permit the synchronization of onboard sensors and the real time transmission of housekeeping data. Strain, pitot probe, and positional data obtained from the GPS/INS will likely be stored using non-volatile flash memory.

3.10 Final Preliminary Design Configuration

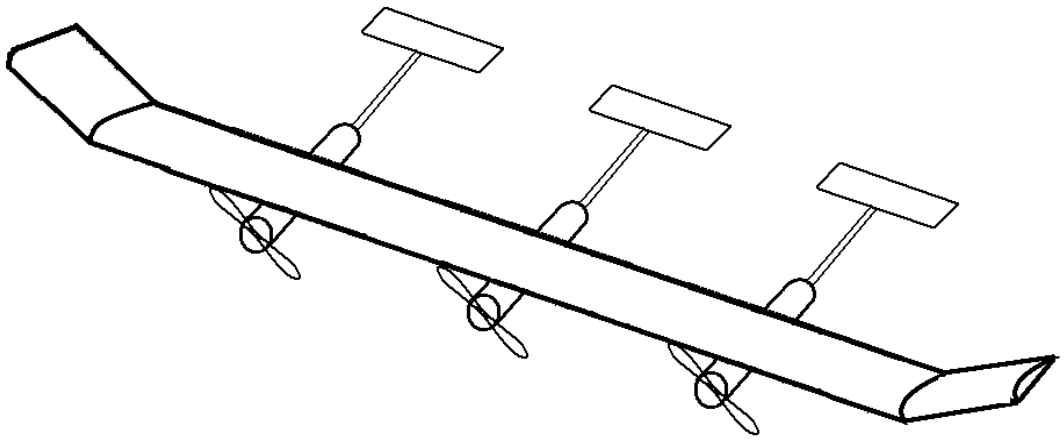

Figure 15. Final Preliminary Design Configuration

Figure 15 above shows a rough outline of the final design configuration. The aircraft's wings will be built using multiple 1-meter wing modules using a reflexed airfoil. The two end wing modules will be given a dihedral in order to increase the lateral stability of the aircraft. The wings will utilize a "wing box" to carry the structural and aerodynamic loads of the wing and will be built of E-Glass. The aircraft's fuselage will be distributed throughout the aircraft in order to reduce point loading. Each fuselage will contain an electric motor powered by a battery contained within the fuselage. Additionally, a rear-facing boom with an elevon will be installed on the fuselage in order to avoid using onboard ailerons that would unpredictably stiffen the wings. The number and size of the elevons would be overdesigned so that the ground or onboard controller would be able to excite certain structural modes for data collection purposes. Strain

gauges would be mounted on multiple locations on the wing box for each wing module in order to collect data to validate the aforementioned nonlinear codes. Five-hole pitot probes will be used to gather accurate angle of attack and relative wind velocities at each wingtip and near the center of the aircraft outside the prop wash of the central propeller. Multiple SBCs will be installed in the fuselages to collect, store, and transmit data from both the scientific and housekeeping sensors.

IV. Current X-HALE Design and Construction

4.1 Current Design Configuration

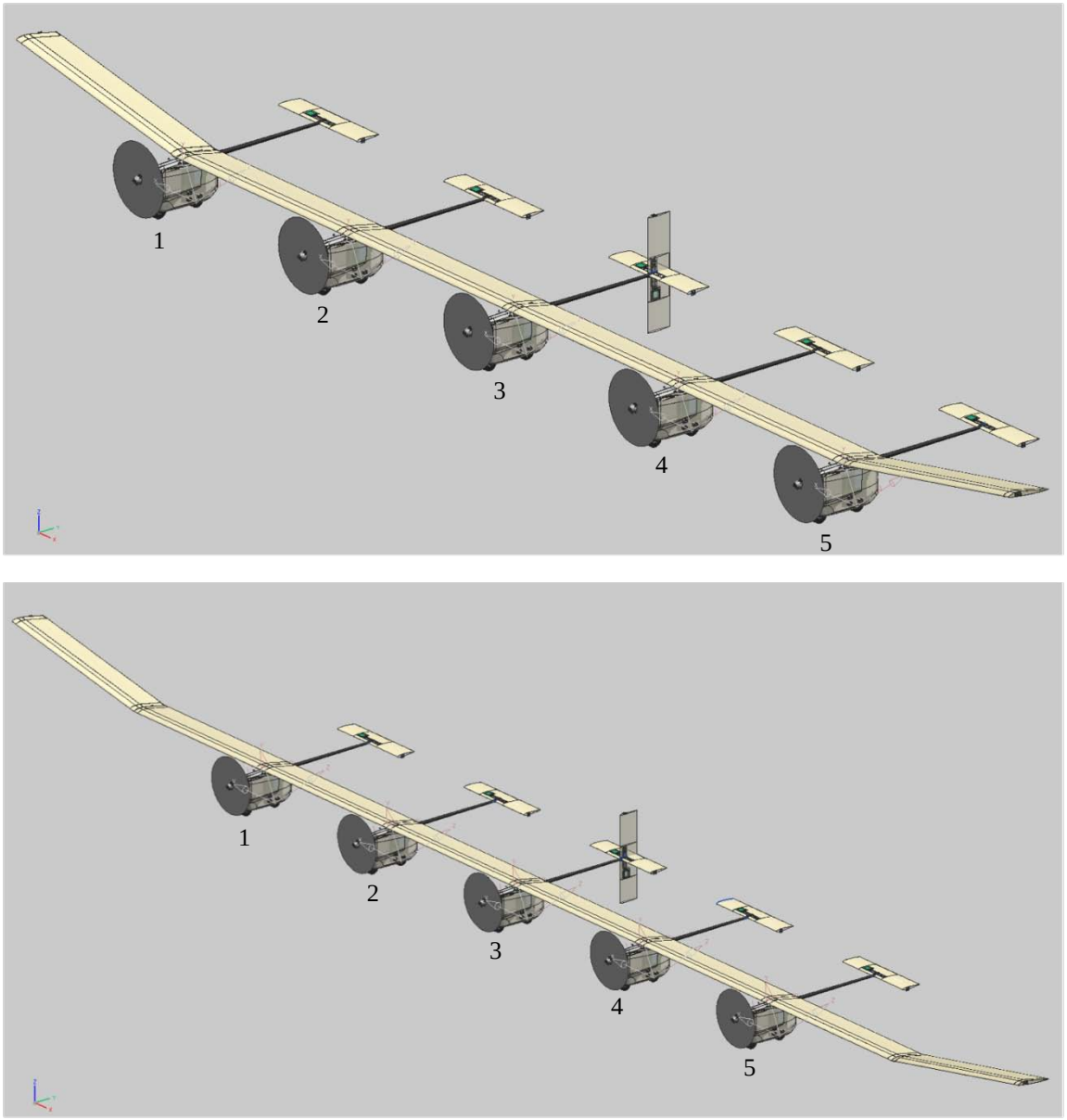

Figure 16. X-HALE: 6 Meter FTV (Top) and 8 Meter ATV (Bottom) [29]

X-HALE's current design is shown above in Figure 16 above. To recap, the FTV is designed primarily to test X-HALE's flightworthiness while the ATV is designed to collect data for code validation. The specific design choices for each subsystem will be

discussed in the upcoming sections, but overall, X-HALE's design remained true to the preliminary design configuration. Both the ATV and FTV configurations include five fuselages, each mounted to a joiner block that connects two wing modules. Each wing module remains one meter long. Each fuselage contains an electric motor and two batteries, one to power the motor and one to power the electronics contained in the fuselage. Each fuselage contains a SBC and an analog to digital converter module along with several scientific sensors. The number and type of sensors varies between wing module and aircraft configuration and will be discussed in the sensor section of this chapter. Table 3 below summarizes X-HALE's characteristics.

Table 3. X-HALE's Characteristics [29]

Wing Span	6 m or 8 m (19.7 – 26.25 ft)
Chord	0.2 m (7.87 in)
Planform Area	1.2 m^2 (3.93 ft^2)
Aspect Ratio	30 or 40
Wing Module Length	0.96 m (3.15 ft)
Propeller Diameter	0.3048 m (12 in)
Gross Takeoff Weight	11 or 12 kg (24.25 – 26.46 lb)
Power/Weight	30 W/kg
Airspeed	12-18 m/s (26.84 to 40.26 mph)
Max Range	3 km (1.86 mi)
Endurance	45 min

Currently, the X-HALE program has manufactured the majority of flight components and is proceeding with integrating these components and developing software for the networking of the onboard computers. The following sections will describe the design and construction of those individual components.

4.2 Wing Design

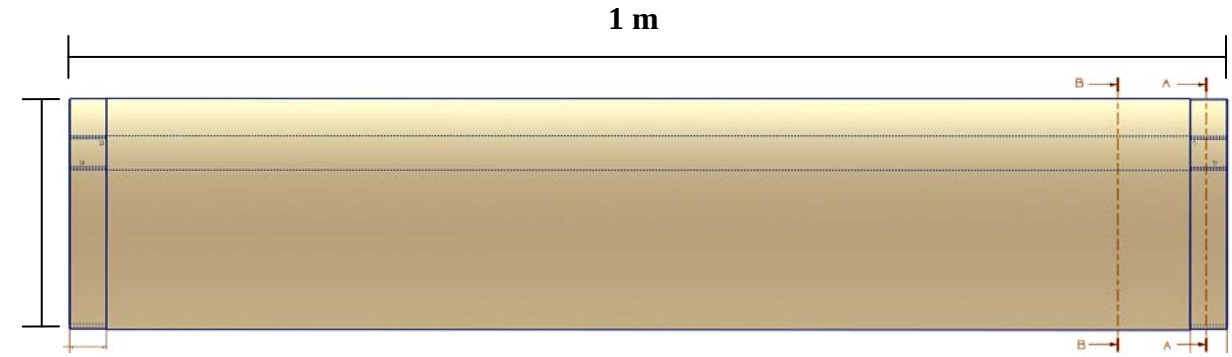

Figure 17. X-HALE's Current Wing Design [5]

For the purpose of transportation, ease of construction, and due to the limitations of the University of Michigan's autoclave, it was decided that the wing be split up into one meter sections. Each wing module has an identical cross section. Figure 17 above shows the design of X-HALE's wing modules. Each wing module has a 3.175 cm recessed portion of the wing designed to fit a fiberglass sleeve (Figure 18). This sleeve helps to transfer torsional loads that would have otherwise been transferred between wing sections via the aluminum joiner block. Both the joiner block and the fairing L-Bracket will be discussed in further detail in the upcoming sections.

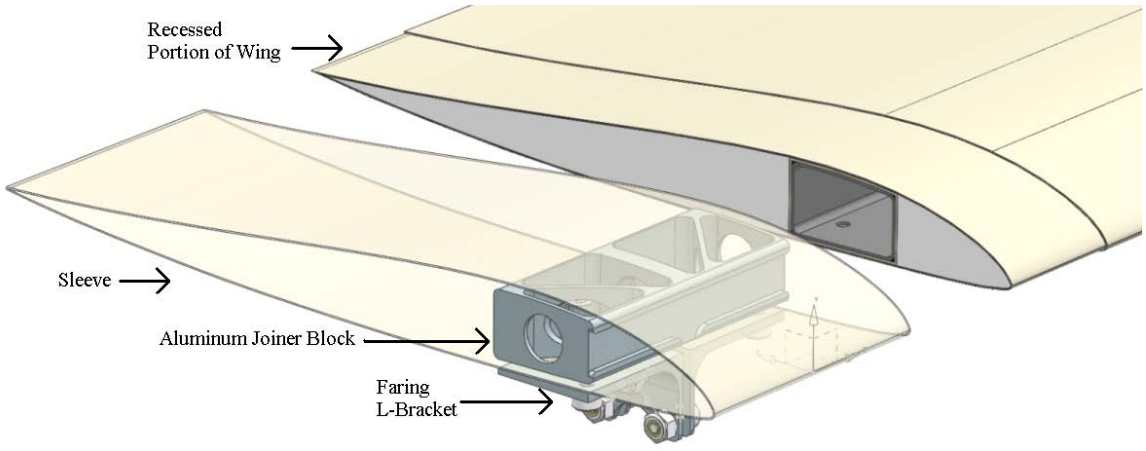

Figure 18. X-HALE Airfoil with Wing Box Highlighted [5]

X-HALE's wings are composed primarily of Hexcel E-Glass 120/F155 prepreg fabric and Rohacell Foam. Hexcel E-Glass 120/F155 prepreg fabric was chosen for ease of construction for both the wing skin and the wing box and also due to its well documented material properties. The physical characteristics of Hexcel E-Glass 120/F155 can be found in Appendix A-3. This fabric was wrapped around a block of Rohacell 31-IG high temperature foam, the characteristics of which can be found in Appendix A-4. Rohacell IG/IG-F foam was used to keep the airfoil's shape and transfer the aerodynamic loads to the structure. Figure 19 below shows a cross section of the airfoil layup. Sections A-A and B-B correspond to the same sections in Figure 17 above.

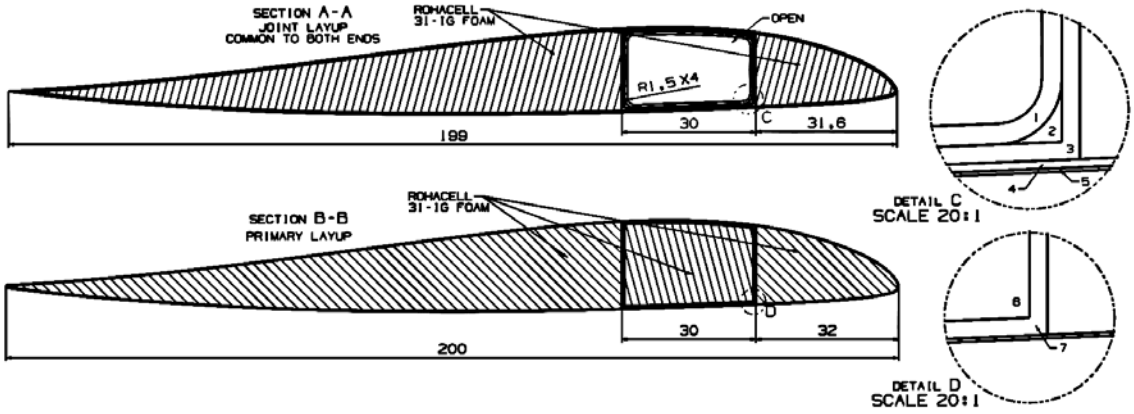

Figure 19. X-HALE EMX-07 Airfoil Layup [5]

It was decided that there would be six wing modules each with a chord of 20 cm. The relatively small chord was selected in order to limit the size and cost of X-HALE while ensuring that it would have a high aspect ratio of 30 or 40, depending on the configuration. Each wing module included layers of IM7/997-3 graphite/epoxy unidirectional tape at the wing joint, the data of which can be found in Appendix A-5. This graphite/epoxy tape reinforces the geometry at the recessed wing joint, but does not

help to carry any load that would not otherwise be carried by the joiner blocks, thus preserving the beam-like structure for validation with NAST.

In order to ensure the wings maintained the structural behavior of beam elements while being joined to the other wing modules, a compact joiner block was designed. This joiner block transfers the structural and aerodynamic loads from one wing module to the next without significantly increasing the stiffness of the wing. The joiner block, with the help of a L-bracket, enables the fairings to be mounted to the joiner blocks rather than to the wings themselves, which would possibly compromise the structural integrity of the wing or the wing box. This joiner block also allows for the wiring from the sensors embedded within the wing to pass through the joiner block and into the next wing module or to the fuselage pod below. A drawing of a non-dihedral joiner block can be found in Figure 20. Complete joiner block schematics can be found in Appendix A-11.

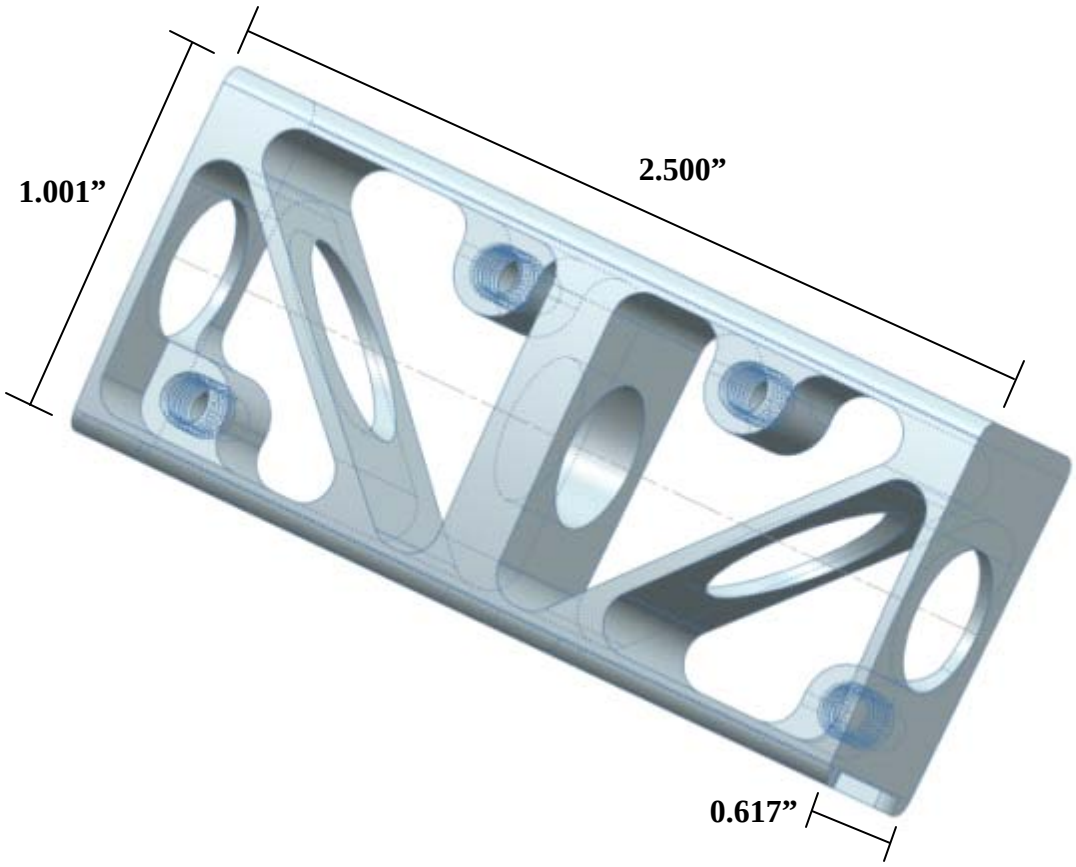

Figure 20. X-HALE’s Joiner Block [5]

Initial attempts at a creating a joiner block that was light, yet strong enough to carry the normal and torsional loads transferred by the wing boxes were met with difficulties. Senatore initially attempted using a basswood joiner (see Figure 20 below), but these joiner blocks caused a large permanent deformation at the joint and a localized bulging of the wing box during 120 lb load testing at the joint[25]. The use of the basswood joiner block also caused a small fracture through the wing box corner and several delaminated fiberglass and carbon fiber plys.

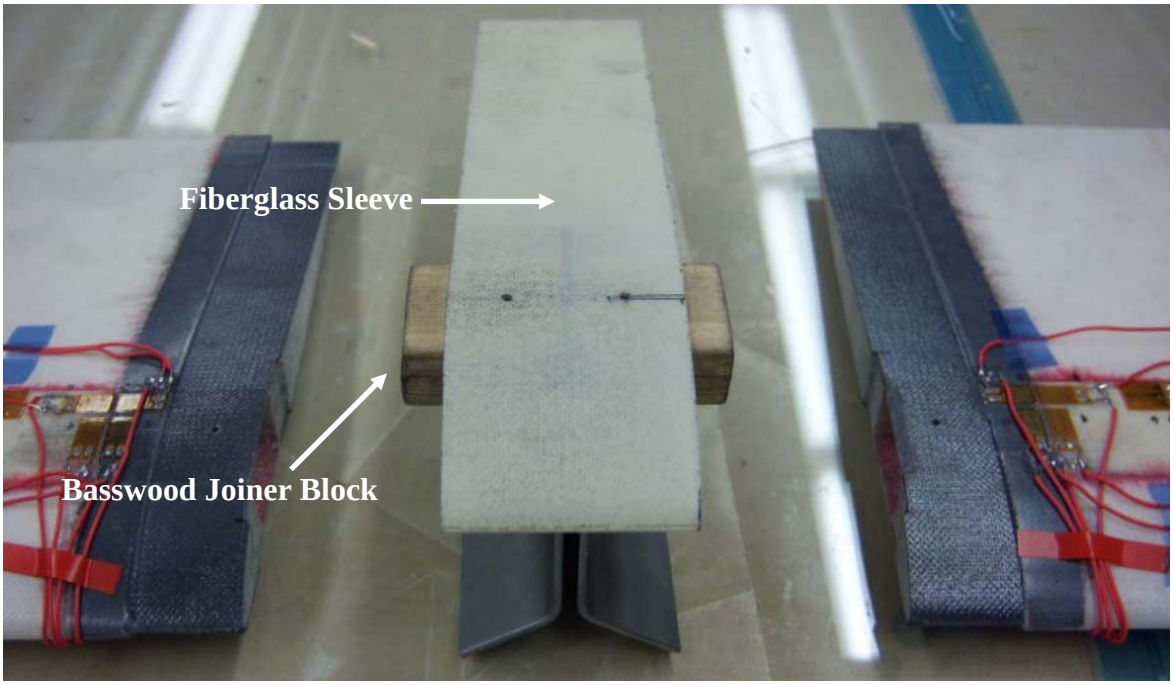

Figure 21. Basswood Joiner Test Setup [23]

The second design iteration utilized a solid carbon joiner block in combination with spruce wood and a 1 mm layer of carbon fiber inside the wing box end of each wing module. See Figure 22 This design attempted to disperse the stress concentration within the wing box through the use of fillets. This design, however, failed to provide the strength necessary for a reasonable factor of safety for X-HALE and still caused localized bulging on the ends of the wing box.

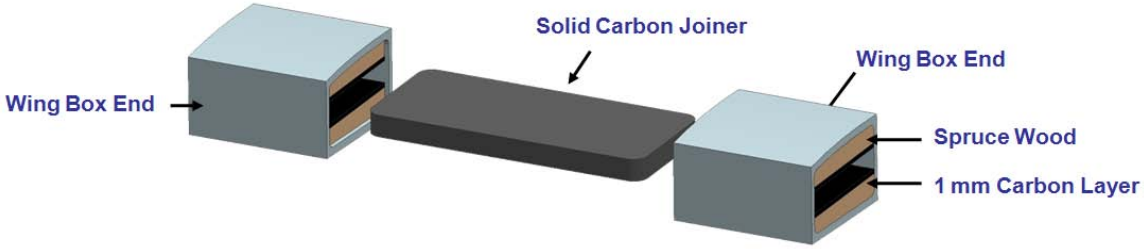

Figure 22. Second Joiner Block Design Iteration [23]

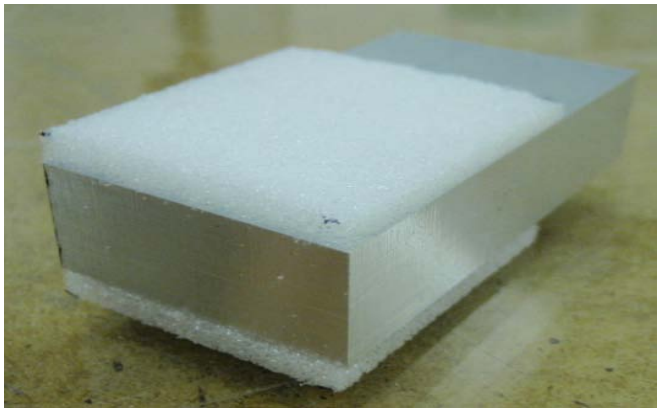

Figure 23. Solid Aluminum Joiner Block [23]

The last design iteration utilized 6061 aluminum and used a solid block for the joiner block (see Figure 23 above). When tested, this joiner block did not cause wing box deformation, but it still caused delamination of the carbon fiber reinforcement as well as the E-Glass surrounding the wing box. The design of the joiner block was modified to use curved edges and corners. Once the design proved that it would not cause delamination of the wing box and carbon reinforcement, the joiner block was then modified to allow wires from the wing mounted scientific sensors into the fairing. Additionally, screw holes were made to allow the mounting of a L-bracket to support the pod. The final design was made as light as possible without sacrificing the strength of the joiner by eliminating unnecessary mass. Figure 24 shows a manufactured aluminum joiner block.

Figure 24. X-HALE Wing Joiner Block [24]

4.3 Wing Construction

This section will provide detail on the planned and actual construction of X-HALE's modular composite wings.

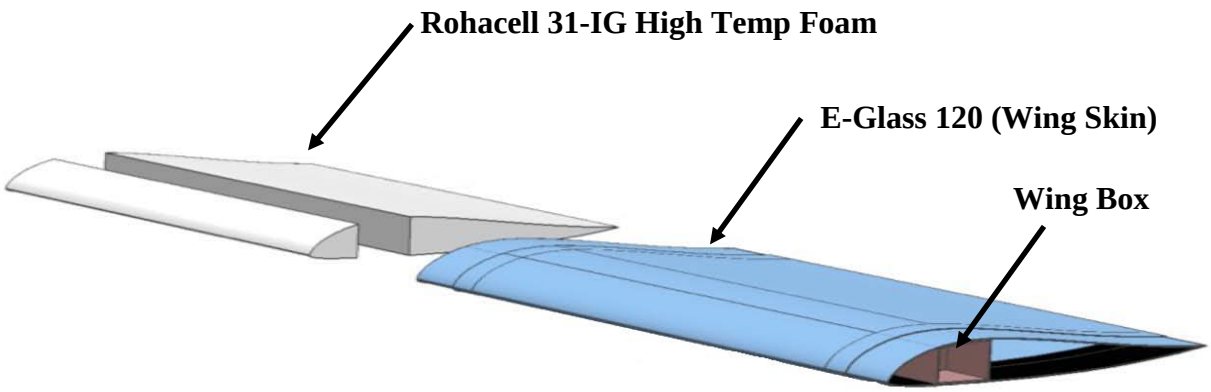

Figure 25. Expanded view of X-HALE's Composite Wing without Joiner Blocks [5]

4.3.1 Wing Box Strain Gauge Installation and Foam Cutting

Figure 25 shows the expanded wing structure of a shortened model of the wings. The Rohacell foam sits inside the E-120 E-Glass shell and adjacent to the wing box. Recall that the foam transfers the aerodynamic loads from the skin to the wing box, and that the wing box carries the structural load of the wing.

Initially, the Rohacell 31-IG foam was laser cut using the University of Michigan's Wilson Center's CNC router to EMX-07 specifications in multiple six-inch sections from the leading edge, the wing box, and the trailing edge. See Figure 26 below for the laser-cut airfoil guides used to guide the laser.

Figure 26. Rohacell 31-IG Foam Airfoil Guides [25]

This manufacturing method was revised by instead using disposable acrylic forms to sand the airfoils into shape. These acrylic forms are cut using a waterjet and provide a more precise airfoil.

With the wing box pieces cut, the individual foam wing-box pieces were glued together to make a one-meter section. The next step was to mount the strain gauges to the wing box foam. Figure 27 below shows the theoretical setup of the out-of-plane, in-plane, and torsional strain gauges.

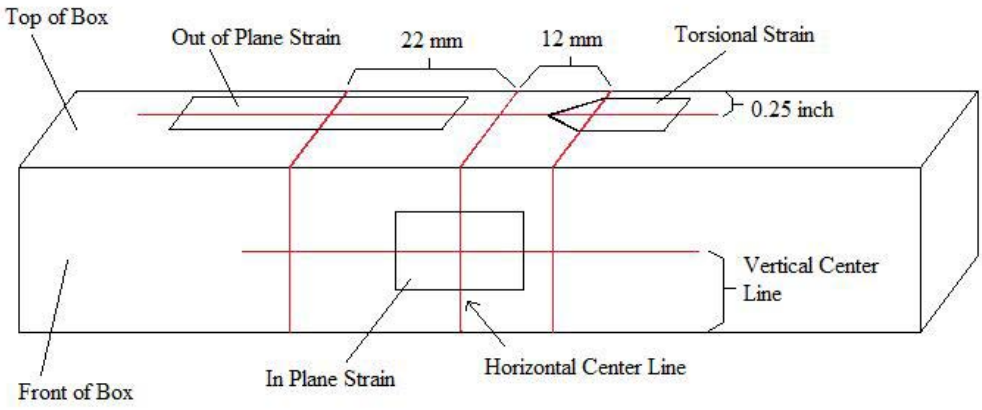

Figure 27. Theoretical Installation of Strain Gauges [21]

The strain gauges were prepared to be mounted on the wing box by soldering the connection wires to the strain gauges and connecting each strain gauge to a small OP-amp on a PCB in order to magnify the signal near the strain gauge to reduce noise. The strain gauges were then glued to the wing box foam. Figure 28 below shows the out-of plane strain gauges and the torsional strain gauges glued to the wing box.

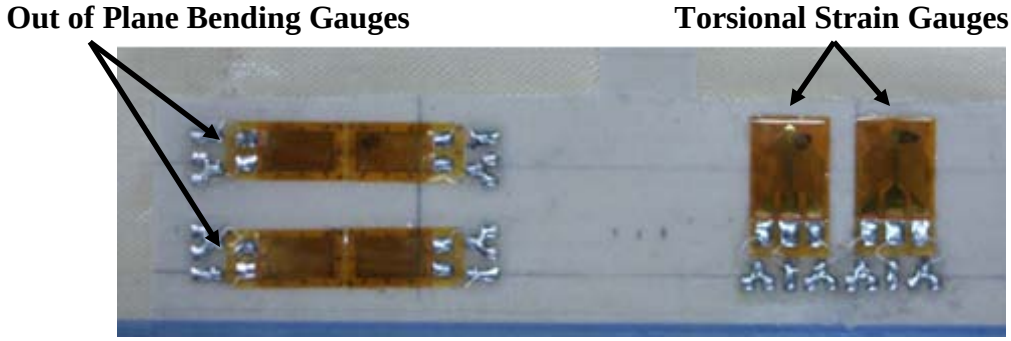

Figure 28. Out of Plane Strain Gauges (Left) and Torsional Strain Gauges (Right) [21]

The wires were then routed internally along the wing box foam using tape strips and cut to length, so that the wires could be connected to the onboard computers within the fairings. The OP-amp PCBs were also glued to the wing box foam where part of the wing box foam had been sanded down so that the wing box would present a flat surface after fabrication. The OP-amps were used to amplify the voltage output from the strain gauges and to reduce signal noise due to the length of wire between the strain gauges and onboard computers. See Figure 29 below for the actual installation of the strain gauges and OP-amps on printed circuit boards (PCBs).

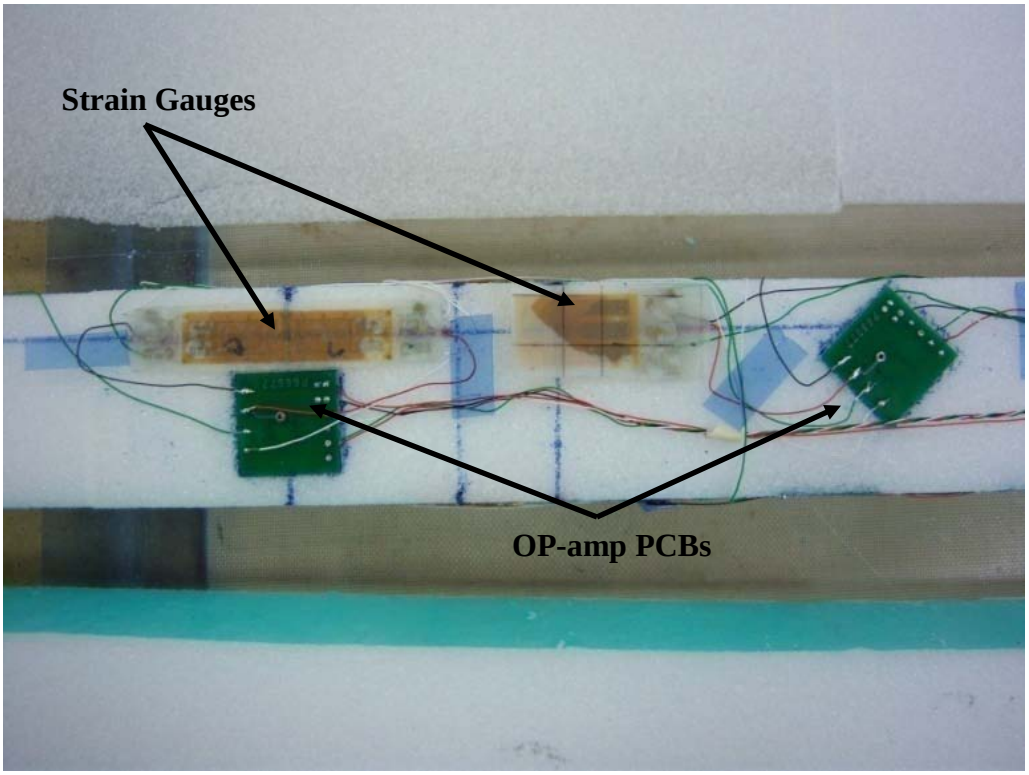

Figure 29. Actual Installation of Strain Gauges [21]

4.3.2 Wing Box Construction

After the installation of the strain gauges, the joiner blocks were prepared to be joined to the wing box. For the two joiner blocks to fit properly on each end of the wing and for there to be no "play," the joiner block blanks were attached to the wing box while the wing box was cured. These joiner block blanks had the same shape as the actual joiner blocks but were solid on the outer edges. Figure 30 and Figure 31 show the theoretical fabrication method used for preparing and incorporating the joiner block with the wing box [23].

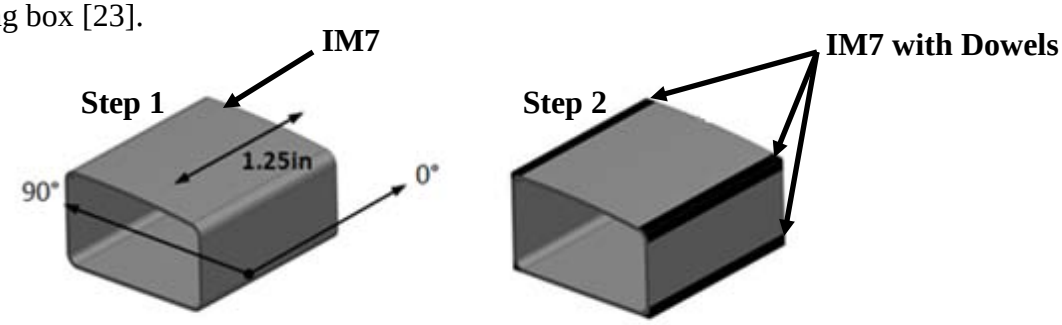

Figure 30. Wrap Unidirectional IM7 Tape Around Joiner Block (Not Shown) and Add IM7 Dowels to Corners of the Layup [23]

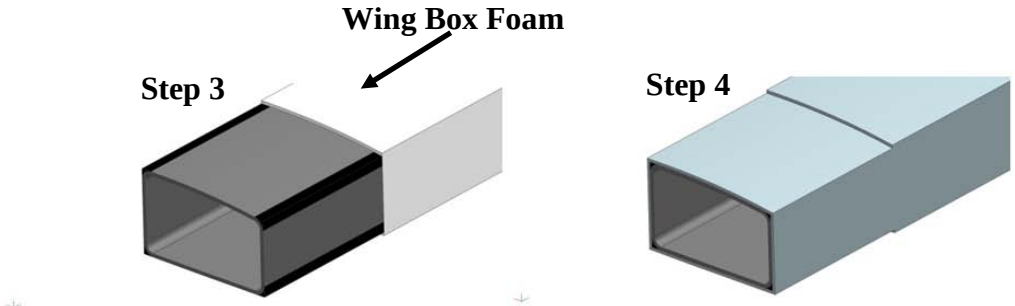

Figure 31. Attach the Joiner Block Layup to the Wing Box Foam and Wrap Assembly in E-Glass Cloth [23]

Table 4. Wing Box Layup Composition [23]

Step	Material	Type	Layers	Thickness (mm)	Orientation
1	IM7*	Unidirectional	5	0.137	90
2	IM7*	Unidirectional	n/a	n/a	0
3	Rohacell 31-IG	Isotropic	n/a	n/a	n/a
4	E-Glass 120	Fabric	5	0.120	0/90

*CYCOM® 381 IM7 uni-graphite 148FAW epoxy (refer to Appendix A-5 for data sheet)

The joiner blanks were first cleaned with acetone and coated with a layer of Freekote and dried. Adhesive film was then wrapped around the filleted end of the joiner blank. A carbon strip 1.5 inches wide was laid on a table and the joiner blank was wrapped tightly around the adhesive film so that there were five layers of carbon fiber. This was repeated for the second joiner block. While ensuring that no bubbles were present in the fibers and all excess material was trimmed from the end of the joiner blank, a rolled carbon fiber rod was rolled to each end of the joiner blanks. See Figure 32 for step 1 (background) and step 2 (foreground).

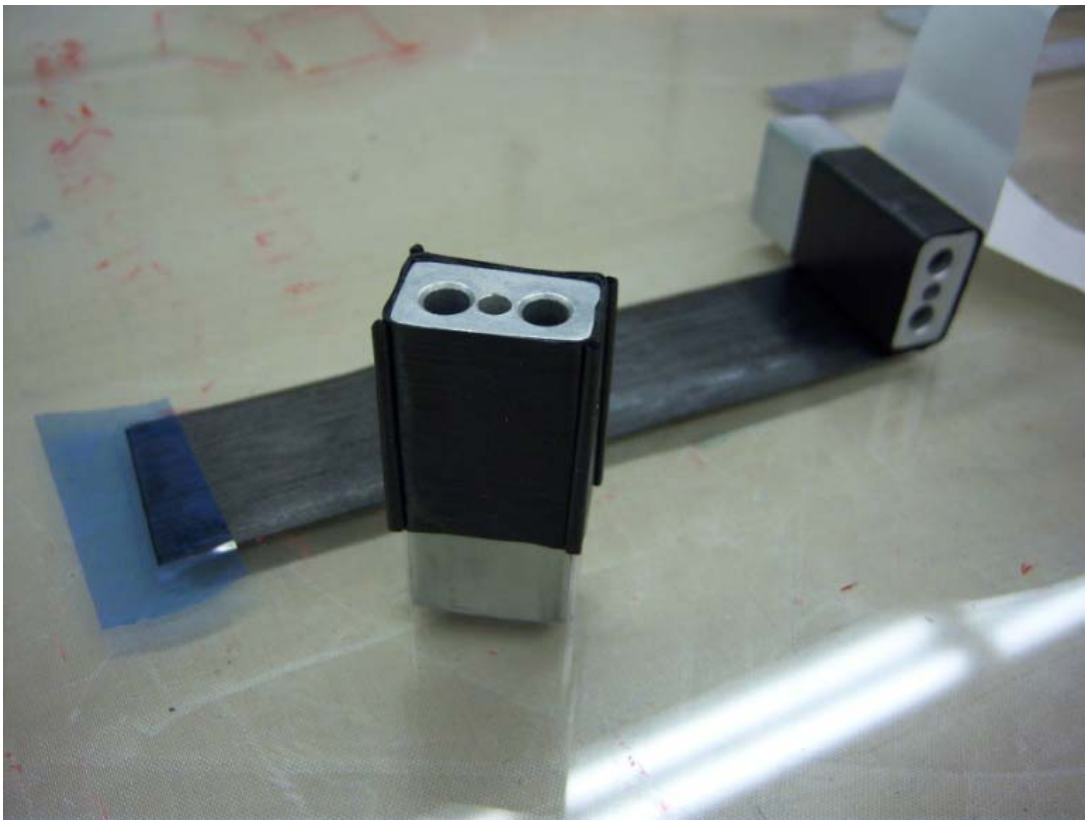

Figure 32. Joiner Blank IM7 Layup [21]

Afterwards, the joiner blanks were aligned to the wing box and any wires (if applicable) were fed through the joiner blanks. The three holes on the blank joiner blanks allowed the blanks to be mounted to the aluminum mold to be discussed. Adhesive film

was pressed down on the carbon layup on the blanks and along the entire wing box on each side. The wing box was then pressed down onto an E-Glass 120 fiberglass sheet. The wing box was tightly rolled along the fiberglass sheet, while ensuring that the joiner blocks stayed in place and no bubbles or any loose fiberglass were present. In order to ensure the wing is correctly joined when complete, two peel ply rectangles were applied over the top and bottom of where the carbon fiber of the blanks met the foam. See Figure 33 below for a picture of a completed wing box

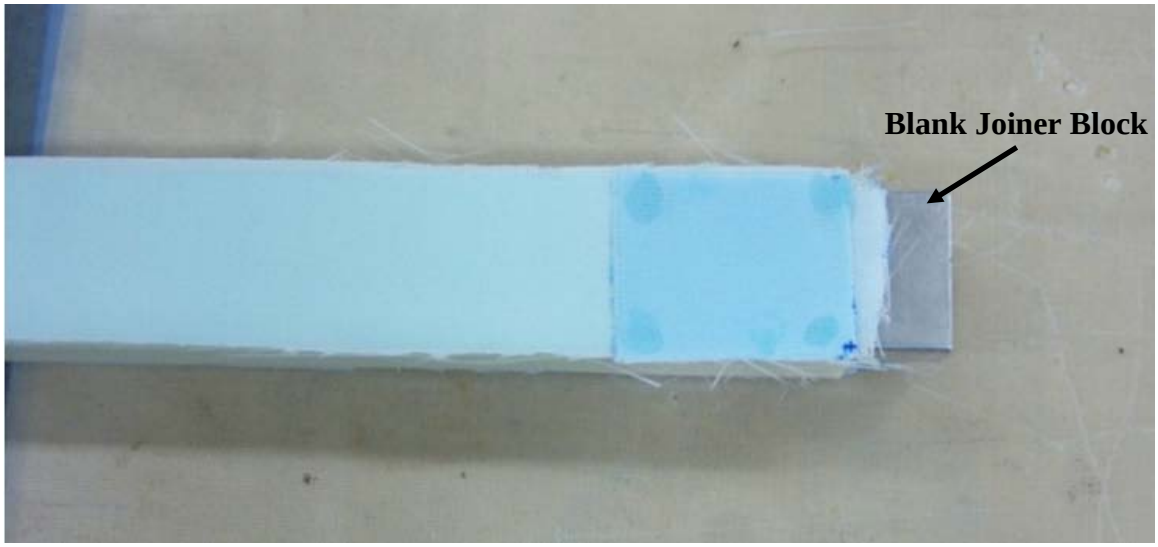

Figure 33. Completed Uncured Wing Box Layup with Joiner Block [21]

With the wing box layup complete and ready to be cured it was placed in the aluminum mold designed and machined by Senatore at the University of Michigan. See Figure 34 for a picture of the aluminum mold measuring (46” x 10” x 2-3”).

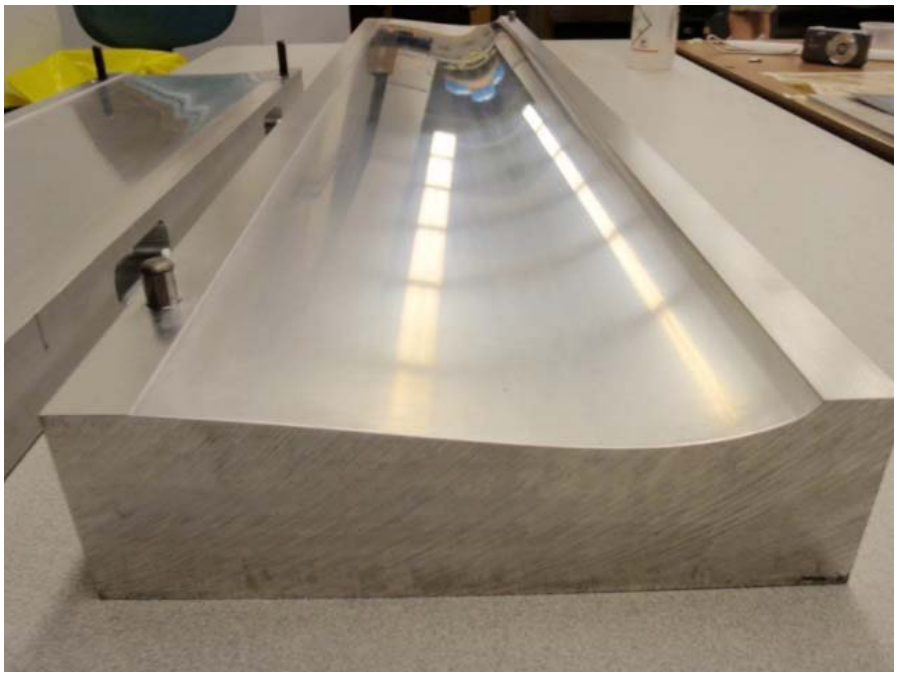

Figure 34. Wing Aluminum Mold [5]

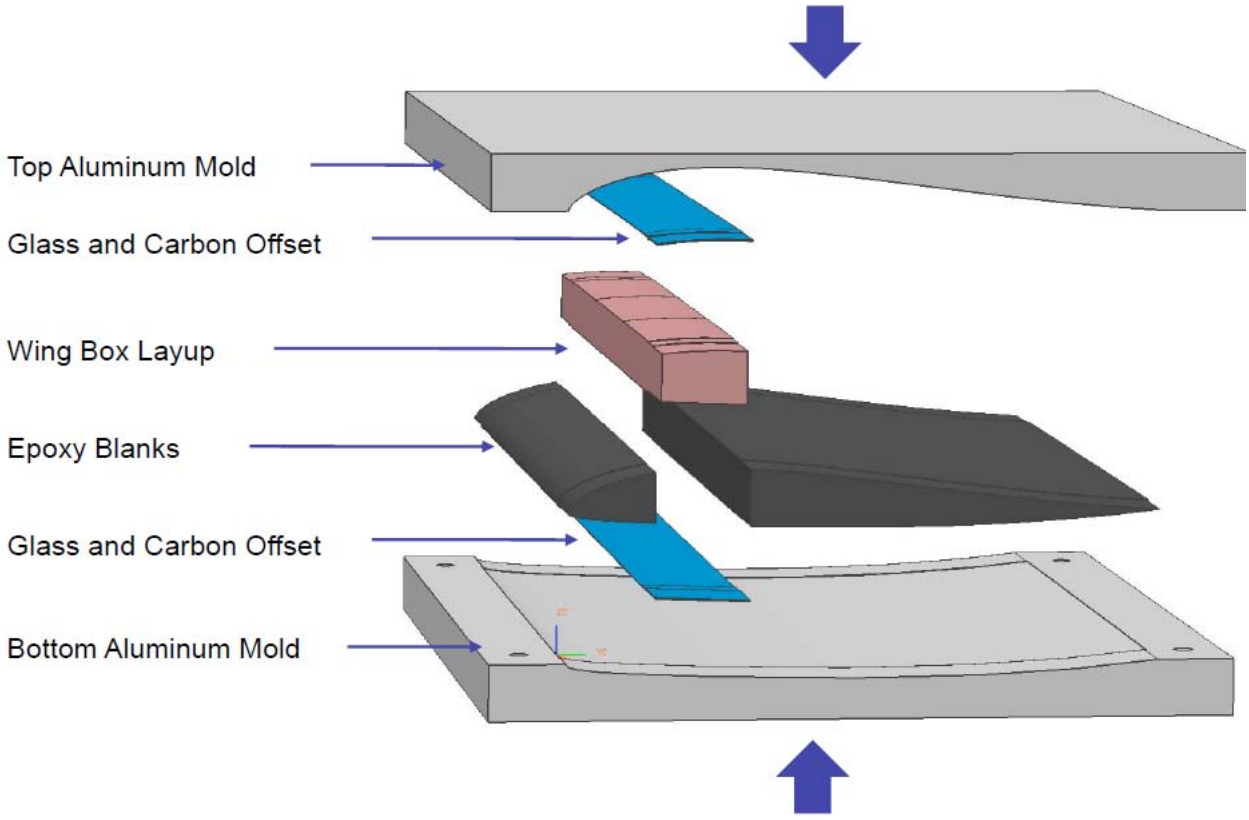

Figure 35. Box Curing Mold Diagram [5]

Figure 35 shows the curing setup used for the wing box. Epoxy blanks and glass and carbon offset pieces were placed around the wing box in order to ensure the proper formation during the curing. The mold was then placed into the University of Michigan's aerospace engineering autoclave, Figure 36, and cured for 3 hours at 250°F and 30 psi. Reference Appendix A-12 for the autoclave's specifications.

Figure 36. The University of Michigan's Engineering Autoclave [5]

4.3.3 Wing Construction

With the wing box completed, the next step was to assemble and cure the wing. Figure 37 and Figure 38 show steps 1-3 of the wing construction. In step 1, the leading and trailing edges constructed of Rohacell foam are added to the wing box via adhesive tape. IM7 carbon fiber tape is added to the edge of the wing in step 2. The final step is to wrap the entire wing in E-Glass 120 fabric [23]. Table 5 shows the materials used for the wing construction.

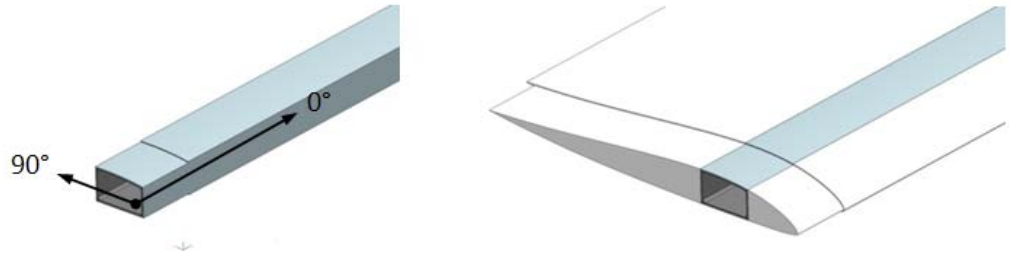

Figure 37. Step 1 of Wing Construction [23]

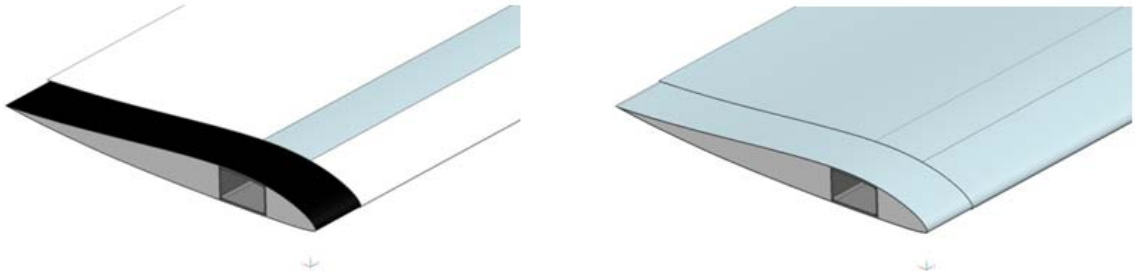

Figure 38. Steps 2 and 3 of Wing Construction [23]

Table 5. Wing Layup [23]

Step	Material	Type	Layers	Thickness (mm)	Orientation
1	Cured wing box	n/a	n/a	n/a	n/a
1	Rohacell 31-IG	Isotropic	n/a	n/a	n/a
2	IM7	Unidirectional	2	0.137	0
3	E-Glass 120	Fabric	1	0.120	0/90

Using the cut and sanded foam leading and trailing edge sections, the first step of wing construction was applying the adhesive film to the thinner sides of the wing box. The leading and then trailing foam sections were then pressed together to form the wing as shown above in step 1. The ends the wings were then reinforced using one layer of adhesive film (45 cm x 3.81 cm) and two layers of zero degree carbon fiber (45 cm x 3.81 cm) in step 2. While the wing sections were tightly held together, the adhesive film strips were applied and then the carbon fiber strips were rolled tightly over the adhesive film for two layers. This process was repeated on the other end of the wing. Figure 39 shows the end of a completed wing before it is wrapped in E-glass.

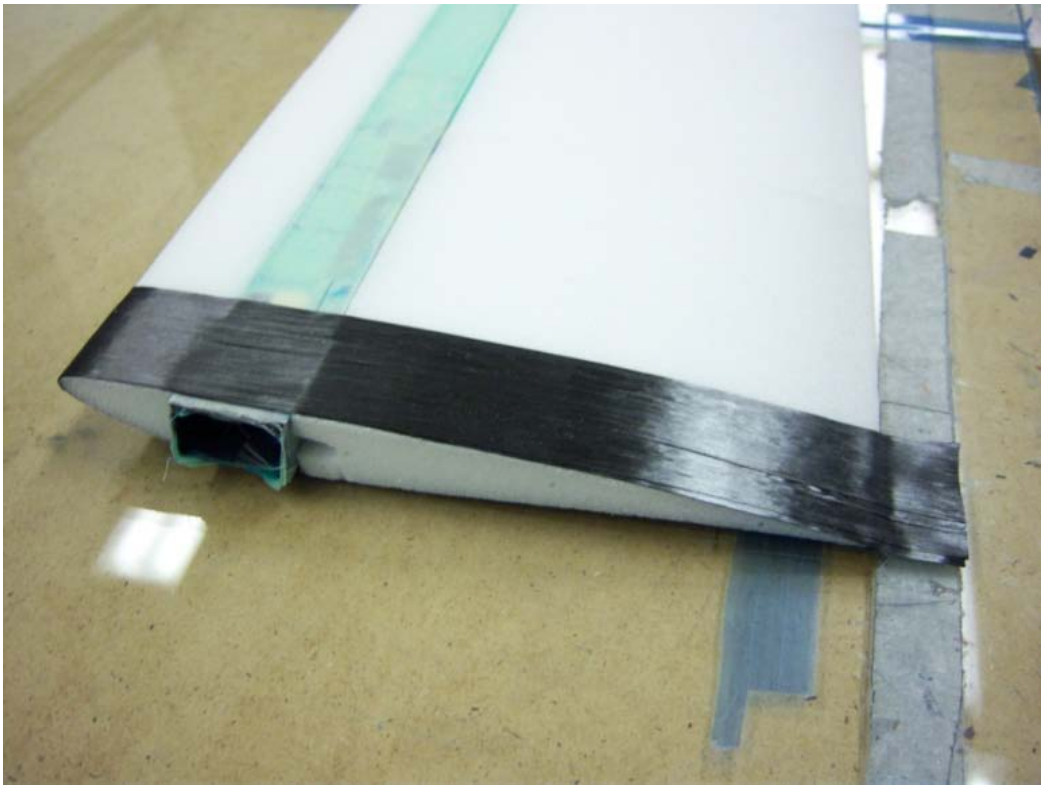

Figure 39. Assembled Wing Prior to Curing [21]

The next step was to peel the top layer of the protective film off the fiberglass fabric that was cut to 1.01 meter x 42.5 cm. The trailing edge of the wing section was

aligned at the very bottom edge of the fiberglass sheet and was lightly pressed down to hold the fiberglass and wing in place. While the fiberglass was held in place, the wing was rolled over and the remaining fiberglass was pulled into place as shown in step 3 on page 50. The fiberglass was then tightly pulled so that no bubbles or gaps were present in the fiberglass. The fiberglass on the trailing edge section was trimmed so that only $1/8^{th}$ of an inch remained, while the carbon fiber reinforcement was trimmed completely.

The final step was to cure the assembled wing. The mold, Figure 34, was first prepared by cleaning the molds, pegs, and blocks with acetone. Once the acetone had evaporated, the wing was coated with a layer of Freekote 700-NC, the material data of which can be found in Appendix A-3. Once the Freekote has been allowed to dry, it was reapplied and then let dry for a total of four times. Next, fiberglass inserts (2 plys IM7) were aligned with an etched line on the molds with the rougher cut side of the fiberglass facing outwards. These inserts, yellow in Figure 40, were taped down with temperature resistant tape, blue in Figure 40. The purpose of these inserts is to ensure the wing maintains the recess near each of the ends so the joiner sleeve can fit over the ends of the wing.

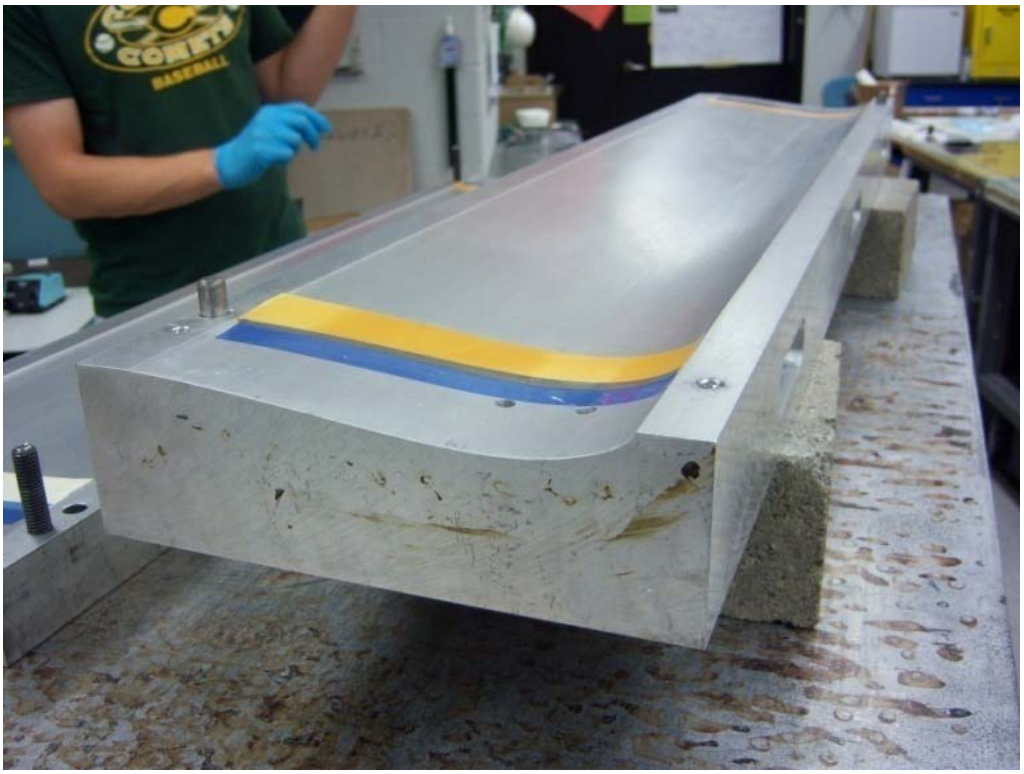

Figure 40. Bottom Aluminum Mold with Fiberglass Inserts [5]

With the mold prepared, the blank joiner blocks were added to the assembled wing and the wing was then carefully placed on the bottom aluminum mold. The top aluminum mold was then lowered and then slowly screwed into place all the while ensuring that the wing is properly orientated. Once the mold was screwed down, the mold was then clamped into place using 6-8 C-clamps to remove any remaining space between the top and bottom molds. Any free wires extruding from the joiner blocks were taped down using temperature resistant tape. The mold was then placed into the autoclave and the autoclave's thermocouple was plugged in and taped to the mold. The autoclave was then shut and cured according to the standard 250°F cure for the 120 E-Glass given by the manufacturer. Once the autoclave and the mold had cooled, the mold was removed and opened. The wing was then inspected and lightly sanded to smooth any rough edges, while ignoring the edges of the wings since they would be trimmed. The

joiner blocks were then removed and the wires were bunched into the wing. A line was drawn one inch from the ridge at each of the tips of the wing and was water cut to create a clean end of the wing. Figure 41 below shows set of completed wing modules. Notice how the wing's foam is divided into six inch sections and the wing tips have carbon fiber reinforcement.

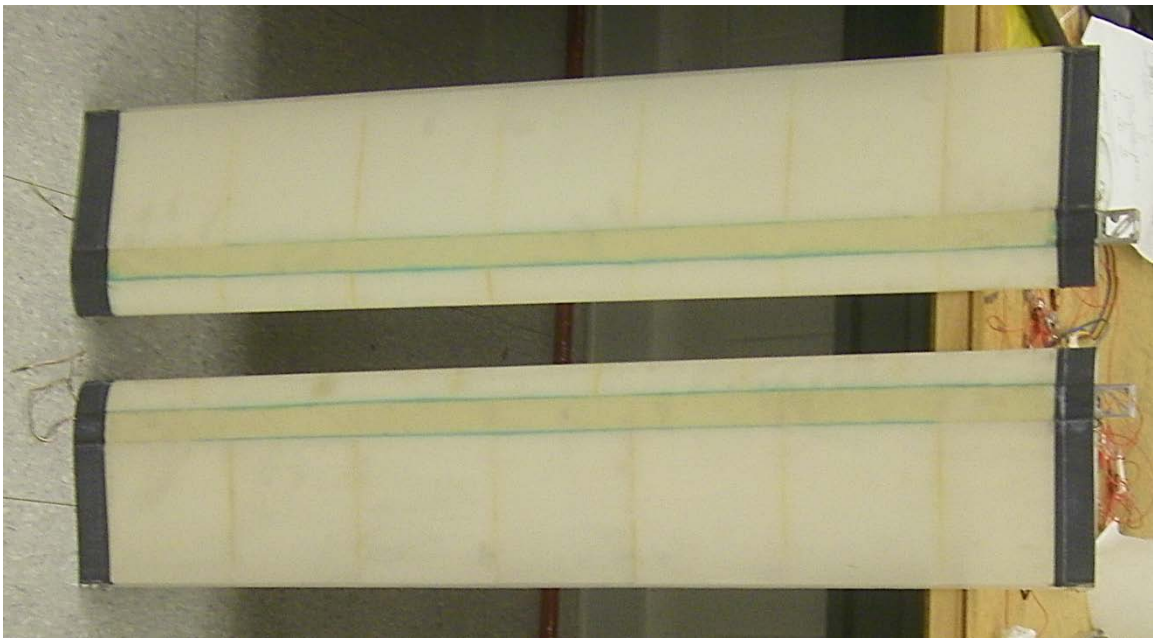

Figure 41. Set of Completed Wing Modules

4.4 Fuselage Design and Construction

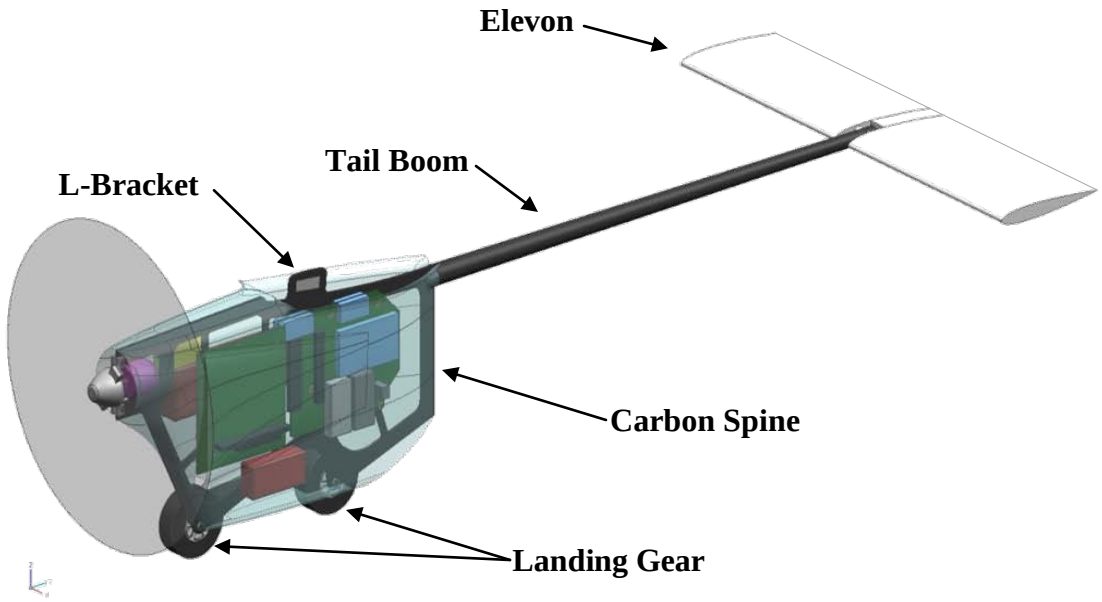

Figure 42. Outboard Fairing with Electronics and Tail Boom Included

Figure 42 above shows an overview of the outboard faring with the landing gear, propeller, internal components, attached boom, and elevon. The design analysis of the fuselage will proceed starting from the L-Bracket and then to the carbon spine. The tail boom assembly will then be discussed, followed a brief overview of the electronics and ending with the landing gear.

4.4.1 L-Bracket Construction

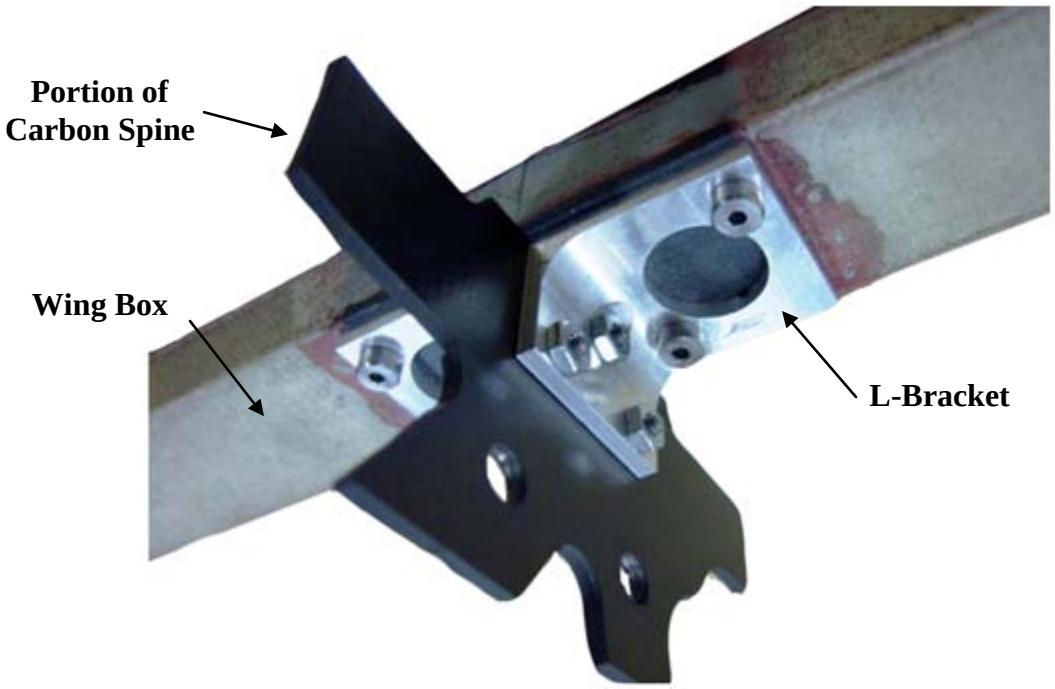

Figure 43. L-Bracket Attachment Sample [5]

Figure 43 above shows the L-Bracket attached to the wing box and a portion of the graphite/epoxy spine. The L-Bracket is made of 6061 aluminum due to its high strength-to-weight ratio and low cost. The joiner block, Figure 20 from earlier, has 4-40 screw holes allowing two contact points with each L-Bracket. Both L-Brackets have three holes to allow for three screw/nut assemblies to mount to the carbon spine. Figure 43 shows an upside down view of the L-Brackets. When fully assembled, the carbon spine will “hang” from the wing box via the L-Brackets.

4.4.2 Carbon Spine Design and Construction

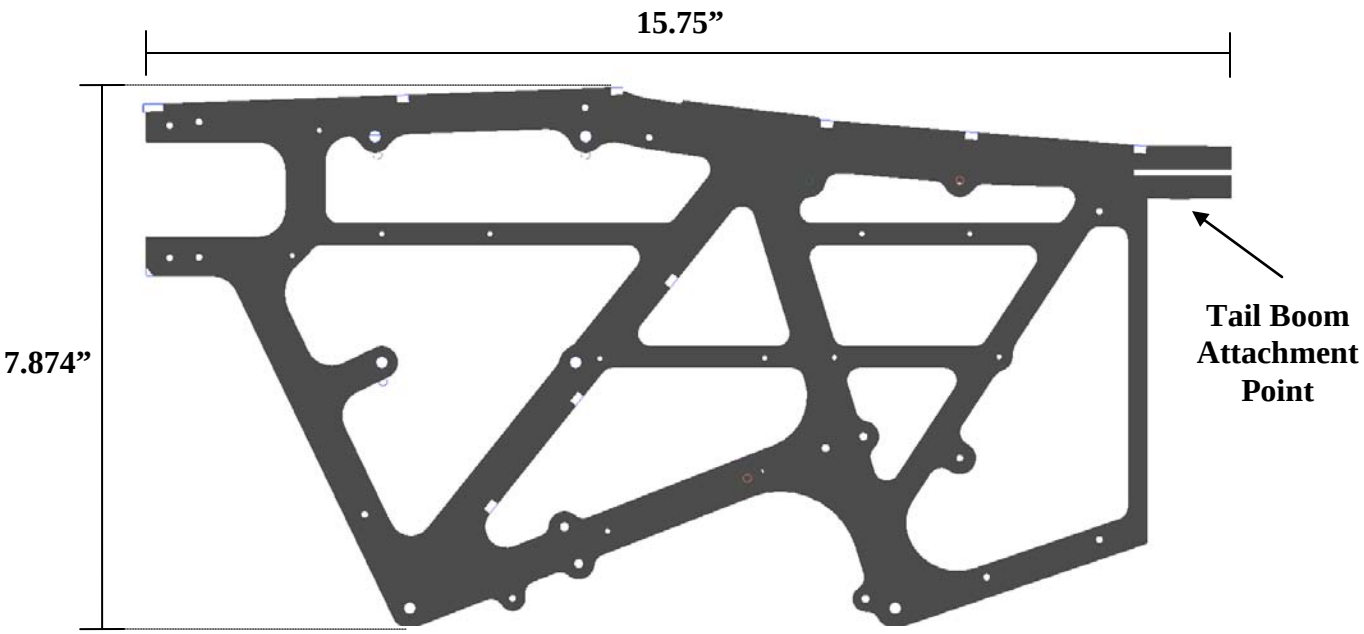

Figure 44. Carbon Spine

The graphite/epoxy spine is composed of 22 layers of quasi-isotropic carbon fiber layup, totaling 2.5mm thick [4]. A cured carbon fiber plate was cut using a using a water cutter to specification according to the CAD model in Figure 44. The design of the spine was driven by several factors: transferring the aircraft’s load to the landing gear while on the ground, supporting onboard electronics, transferring the thrust from the motor to the wings, and providing a mounting point for the tail boom. Figure 45 and Figure 46 show an internal view of the central fairing. The electronic components shown in the figures will be described in the electronics section in this chapter.

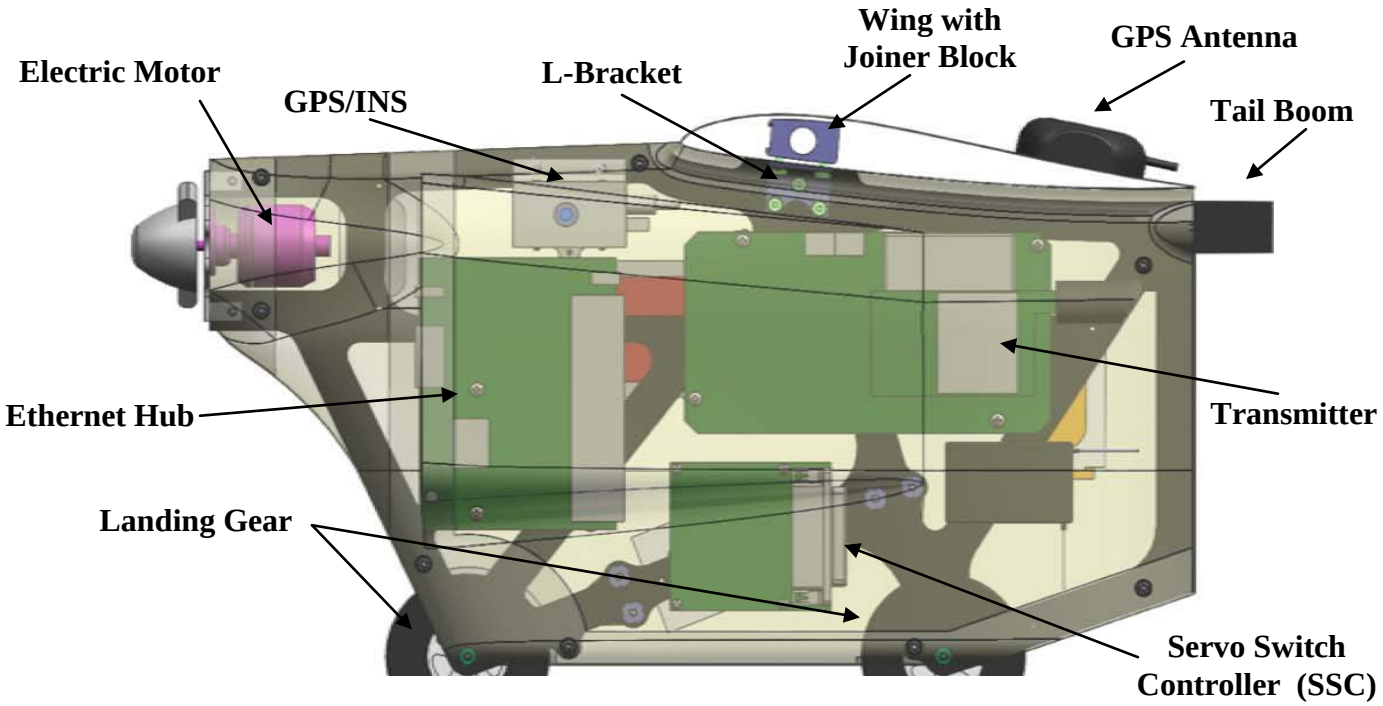

Figure 45. Spine with Internal Components (Right View) [5]

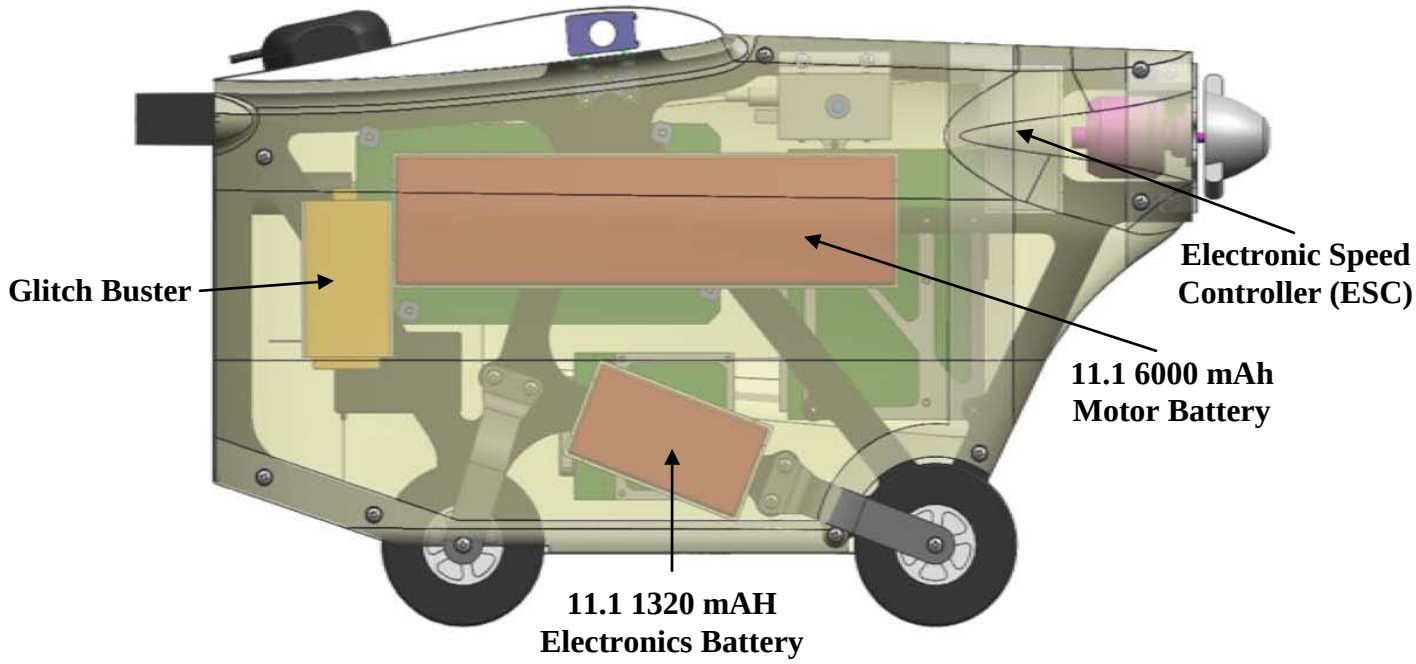

Figure 46. Spine with Internal Components (Left View) [5]

4.4.3 Faring Design and Construction

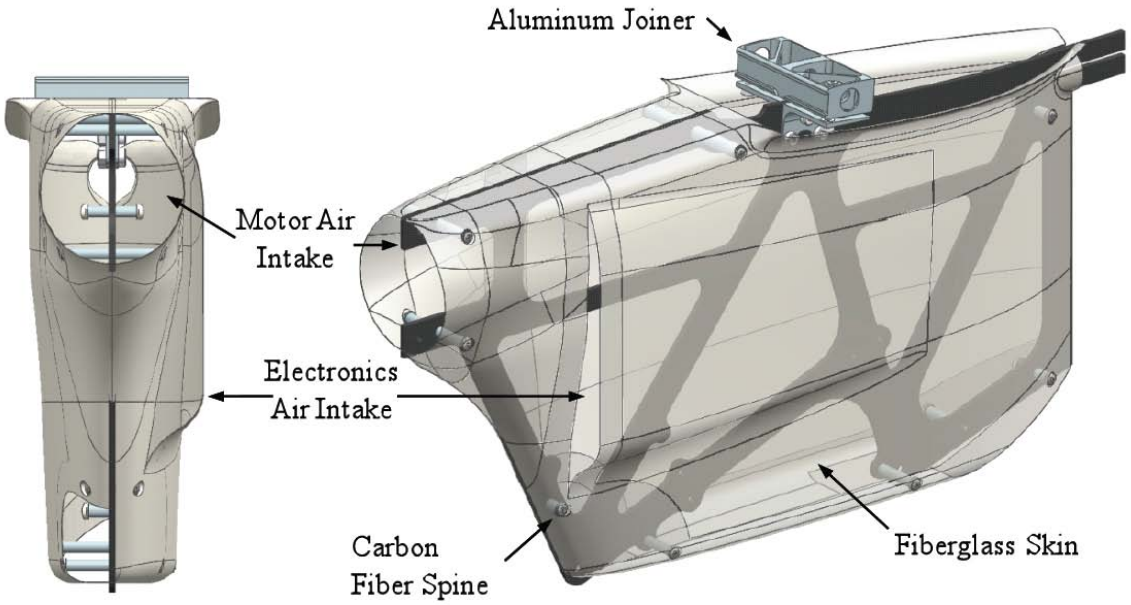

Figure 47. Final Fuselage Fairing Design [6]

Figure 47 above shows the carbon spine with the fiberglass shell. The fiberglass fairing shell is composed of three layers of pre-impregnated fiberglass and is shaped as a NACA 0010-66 airfoil modified to 18% thickness. The design of the shell was driven by the size of the electronic components as well as creating a streamlined fuselage to reduce the aircraft's parasitic drag. Detailed schematics of the fairing can be found in Appendix A-14.

Figure 48 and Figure 49 show a visual progression of the construction of the fairing shell. Senatore created a mold for the fairing shell in order to ensure identical shells for each fairing pod. The mold was first cleaned with water in step 1. Next, three layers of pre-impregnated fiberglass were cut into a two-dimensional projection of the mold and laid up together on a hard surface to help eliminate all air pockets and creases.

Finally, the mold and fiberglass layup was vacuum bagged and cured in the autoclave at a pressure of 80 psi and temperature of 250°F for three hours

Figure 48. Fairing Shell Construction Step 1

Figure 49. Fairing Shell Construction Step 2

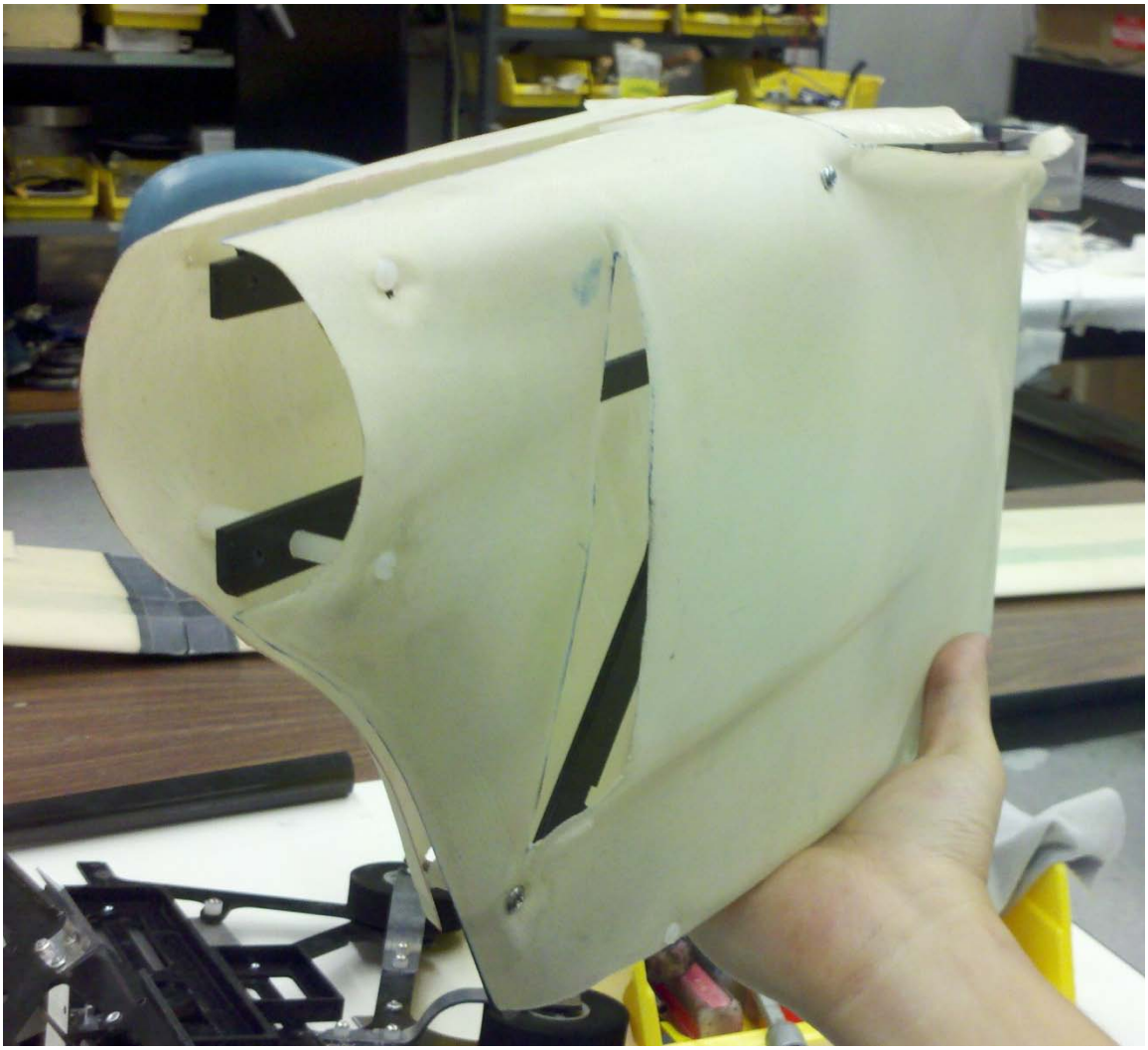

Figure 50. Completed Fairing Shell with Carbon Spine

Figure 50 above shows both sides of the completed fairing shell. The shell is joined to the carbon spine through the use of plastic pin connectors and screws. The large openings in the shell allow for airflow through the pod for electronics cooling.

4.4.4 Tail Boom and Landing Gear Design and Construction

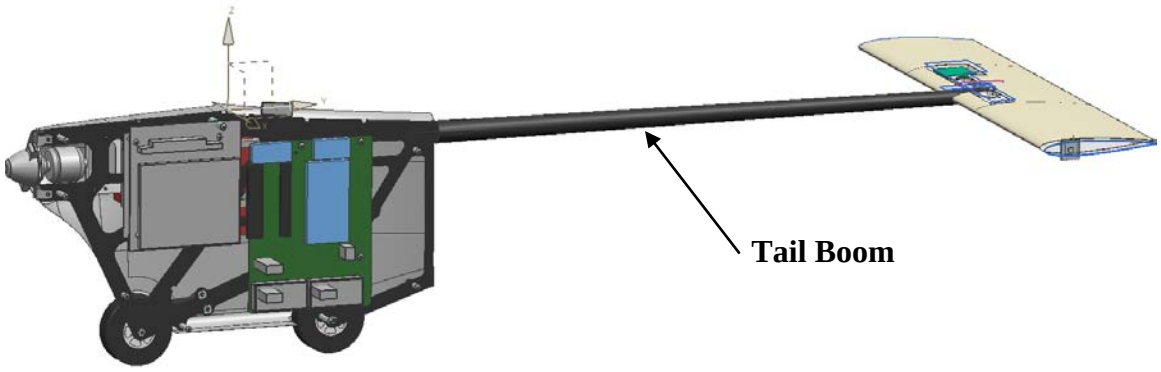

Figure 51. Fairing Pod with Tail Boom and Elevon

The tail boom was available commercial off the shelf (COTS) and was cut lengthwise to specifications. See Appendix A-16 for fairing and tail boom dimensions. Initially the tail boom was placed over the tail boom extension on the carbon spine as shown in Figure 44 and Figure 52. However, it was determined that a hard landing would create enough stress to break the spine, requiring the construction of an entirely new spine. A design change was made to screw the tail boom extension onto the spine which the tail boom would be attached to. In the case of a hard landing, the tail boom attachment would fracture rather than the fairing carbon spine.

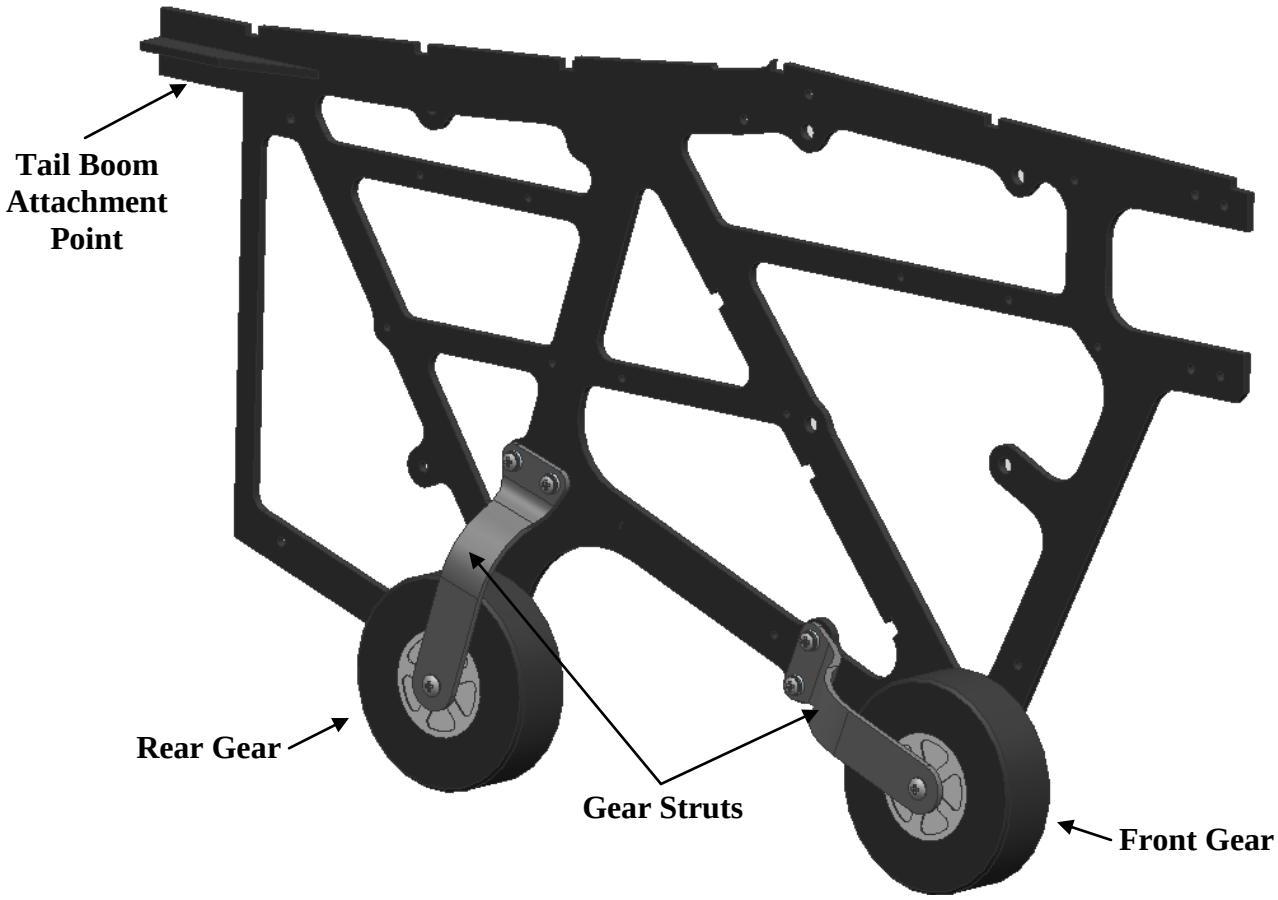

Figure 52. Carbon Spine with Landing Gear

Figure 52 shows the carbon spine with landing gear. The wheels used are Dave Brown WH25 Lite Wheels composed of light weight, low bounce, durable foam. Further data regarding the wheels can be found in Appendix A-23. While these wheels are designed to absorb the majority of the impact forces from a "hard landing," the gear struts attached to the carbon spine also absorb a portion of the impact forces.

4.5 Propulsion Design and Implementation

Figure 53. PJS 1200 ART (Left) and Example 12” x 6” Model Propeller

Based upon initial mass and drag calculations, the design team selected an electric motor build by the CzPJSza Corporation. These motors, built in Czech Republic, use neodymium magnets and are highly reliable. The motors require a maximum of 75W of power and will utilize the fairing’s electronic air intake vents for cooling. Engine dimensions and additional specifications can be found in Appendix A-15. Each motor is paired with a 12” x 6” standard RC model propeller.

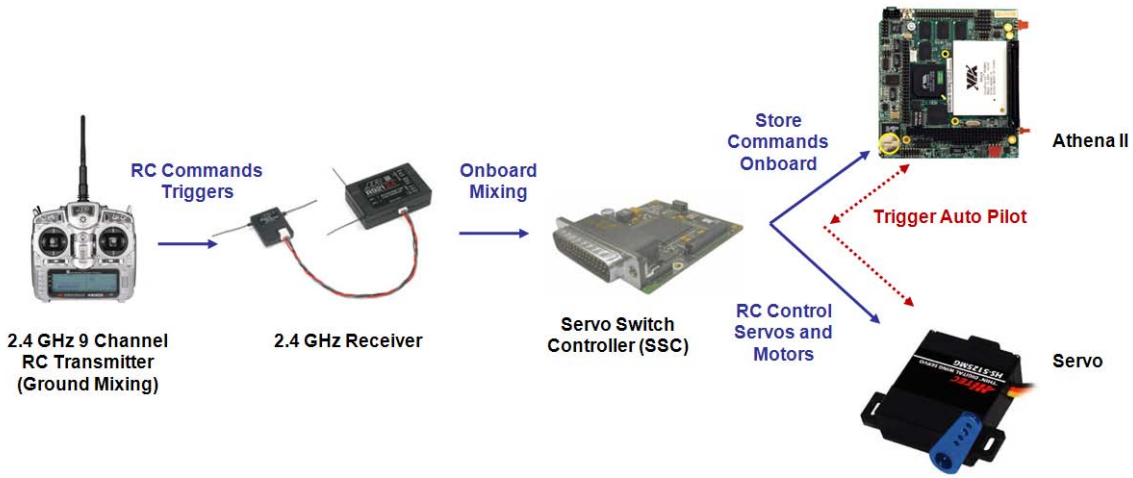

Figure 54. X-HALE Flight Control Diagram [25]

Figure 54 shows a diagram of X-HALE’s flight control process. Commands are inputted into a JR X9303 transmitter (Appendix A-20) and are received by four JR R921 (Appendix A-21) receivers in each of the outboard fairings. The control scheme has been carefully programmed on the transmitter so that the pilot does not need to individually

manipulate the controls for each motor and tail. An input of forward thrust increases the throttle for all motors. Commands for yaw causes differential thrust for the outboard motors. Pitch commands actuate tails 1 and 3, and roll commands use all tails differentially or in a 2-4 and 1-3 combination. See Figure 16 for fuselage pod numbers. These commands are then sent to the servo switch controller that sends the commands to be stored on the Athena II SBC or sends the commands directly to the servos and motor ESCs (electronic speed controllers). The servos placed in the elevons will be described in section 4.6. Each faring contains one ESC that regulates the current sent to the motor.

Each motor is powered by a Thunder Power 11.1 V 6000 mAh battery. Assuming a 45 minute endurance, 75W power draw, and 100% duty factor, the engine would require 56.25 Wh. This would cause a depth of discharge of 84% for the motor batteries. While a larger battery would increase the available power for the mission, additional weight would increase the takeoff roll, increase fuselage point loading, and reduce the space available in the fairing. The designers chose to use the 6000mAh battery despite the high depth of discharge (DOD) due to the considerations mentioned and also due to the fact that X-HALE motors will not be operating at 100% duty factor during the duration of the flight. However, realizing the potential high power draw, X-HALE is not destined to be flight tested in cold environments to avoid premature battery failure. In the case of a battery or motor failure, the aircraft's remote pilot has the ability to immediately turn off power to the remaining motors and control X-HALE in a glide configuration.

4.6 Control Surface Design and Implementation

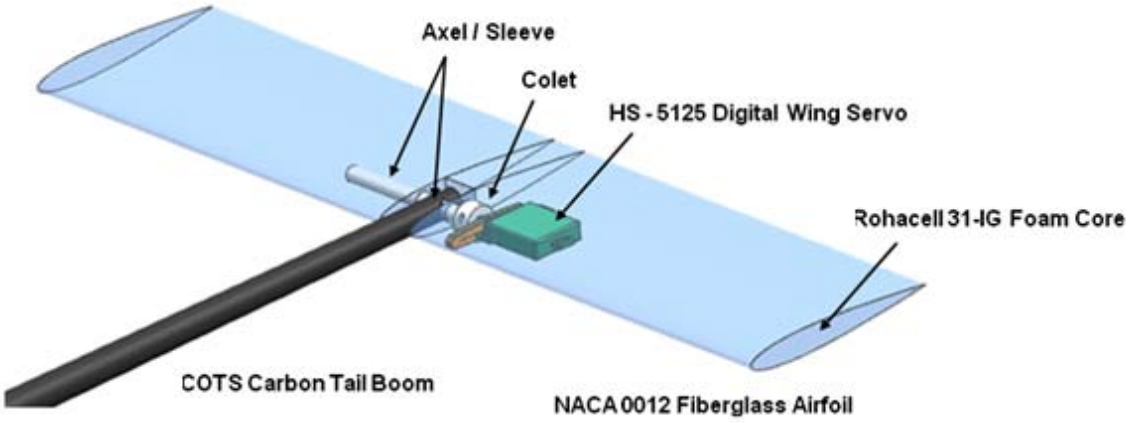

Figure 55. Elevon Overview [29]

It was decided that four booms would be required in order to effectively excite structural DOF for both the 6 and 8 meter X-HALE configurations and to control the aircraft in pitch and roll. Figure 55 above shows the elevon with a portion of the skin cut away to show the self contained servo. Detailed dimensions of the tail can be found in Appendix A-6. The wing profile for the elevon is a NACA 0012 symmetric airfoil. Symmetric airfoils were used due to the predictability of the relationship between their coefficient of lift vs. angle of attack. The booms extending from X-HALE and are placed symmetrically on each half of the wing extending from the fairings closest to the center of the aircraft. Placing the booms nearer to the ends of the wings would be able to more effectively excite the aircraft's structural modes. If X-HALE was placed in a high dihedral configuration the force from the elevon would act normal to the curvature of the wing at the boom attachment. However, since the ground controller or the autopilot would be unable to determine the exact dihedral of the aircraft, controlling the aircraft in this configuration would be more difficult and less accurate. Until a more accurate

control scheme can be developed, X-HALE will continue using near-center mounted elevons.

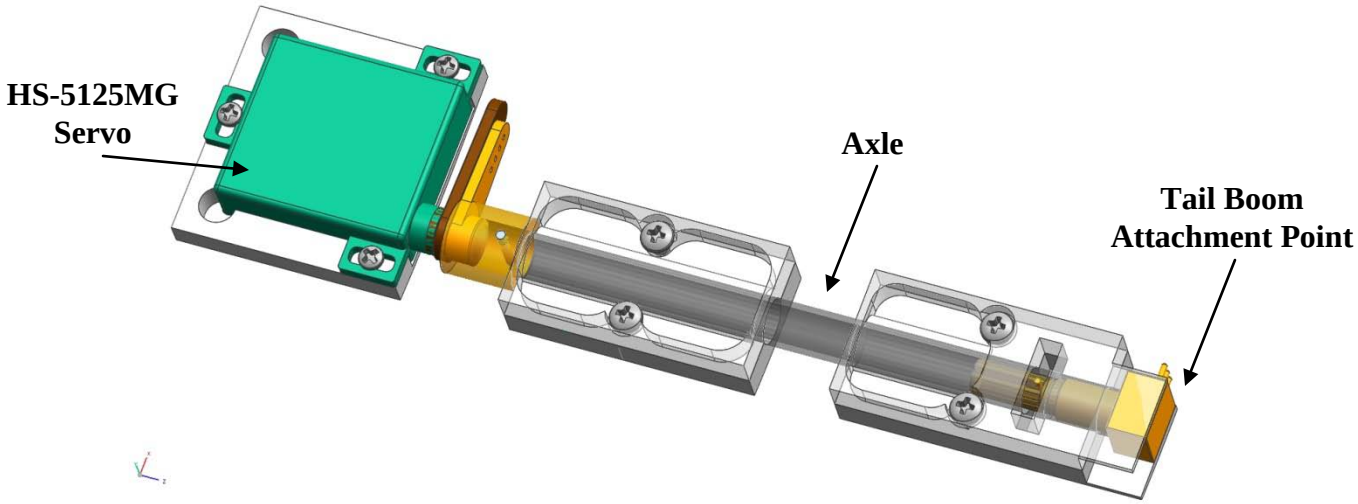

Figure 56. Internal View of Servo [29]

Figure 56 shows an internal view of the servo used to actuate the elevon. A HS-5125MG servo, Appendix A-7, was used for the elevon since it was the thinnest digital servo available at a reasonable price. The servo can be actuated ±45 degrees to the neutral axis, making it more than effective for its use actuating an elevon. The servo is rigidly attached to the elevon via glue to the fiberglass skin. The axle (grey cylinder in Figure 56) is rigidly attached to the boom. When the servo is actuated, both the elevon and the servo move. A servo potentiometer reports back to the controller (human or computer) the position of the elevon. The servo's wiring travels from the corresponding fairing's SBC, through the boom, and within the elevon to the servo. See Figure 51 for a theoretical installation of the tail boom and Figure 57 for a completed elevon.

Figure 57. Completed Elevon/Servo Assembly

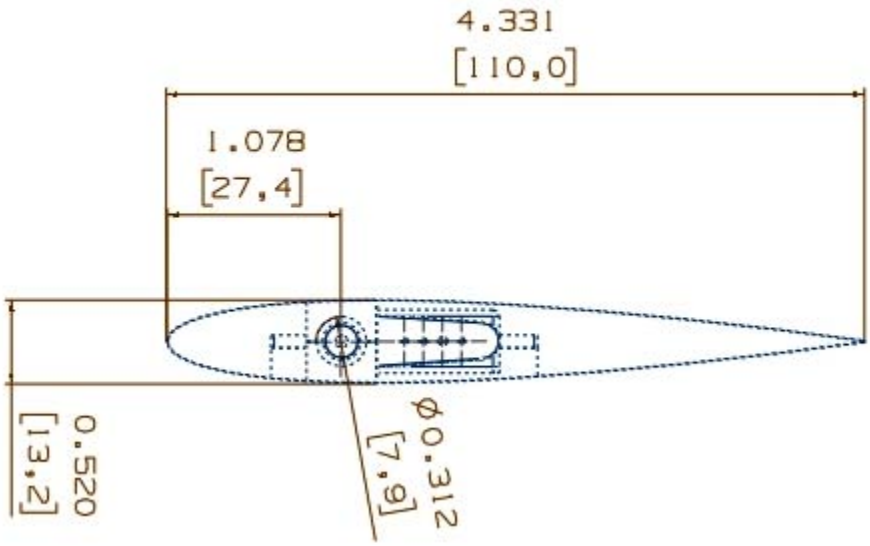

Figure 58. Elevon (Units in Inches, Bracketed Units in mm)

The elevons were created from the same materials as the wing: 0-120 E-Glass and Rohacell 31-IG Foam. Internally, the elevon does not have a wing box and only uses the 0-120 E-Glass for the skin. The elevons were cured in the autoclave using the same process as the wing modules except it only required one cure since there was no wing box. The dimensions for the elevon can be found in Figure 58 above.

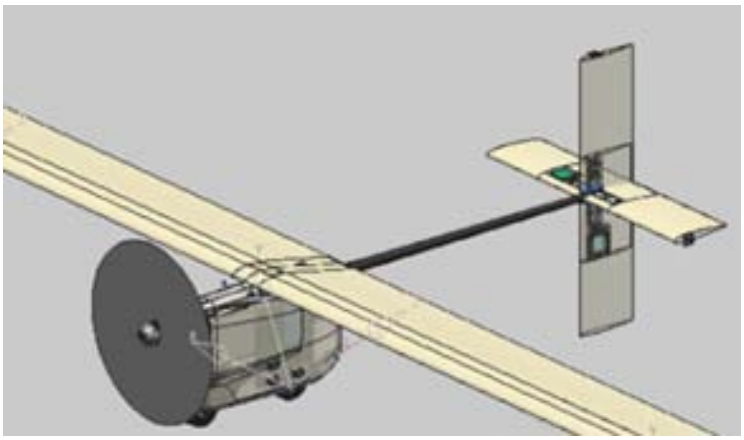

Figure 59. Original X-HALE Center Tail Configuration

Through the use of numerical simulations using UM/NAST, it was discovered that through differential elevon inputs, the aircraft could become unstable in roll [29]. With no vertical stabilizers present on the aircraft, the solution to this problem clearly was to add a vertical tail. However, the addition of a vertical tail would also dampen the very aeroelastic phenomena X-HALE was designed to create. Therefore, the solution was to create a vertical tail that could be intermittently engaged during flight. See Figure 59 above for a zoomed in look at the center tail. The figure shows how the tail can be orientated either the vertically or horizontally. This tail does not have the ability to rotate as an elevon.

The center tail has a similar configuration to the standard elevon shown in Figure 55 with the exception that the tail rotates 90 degrees about the boom's longitudinal axis. Effectively, the horizontal tail becomes a vertical stabilizer. The movement of the vertical tail is controlled by a switch in the pilot's RC transmitter (where typically landing gear up and down is controlled). The vertical surface is activated to enhance lateral stability of the vehicle and to arrest the flexible dutch roll instability.

The numerical simulations also indicated that X-HALE could develop roll instability issues during takeoff and it would be necessary to activate the vertical stabilizer during takeoff. This was not possible with original length of the tail. It was decided that for there to be significant ground clearance for the aircraft's takeoff rotation, the center tail would be cut short on the left side. Since the airfoil is symmetric, it would not create a lateral moment and would only induce a very slight yaw due to the reduced parasitic drag on the left side of the tail. See Figure 60 for the vertical tail design and Figure 61 for the constructed vertical tail.

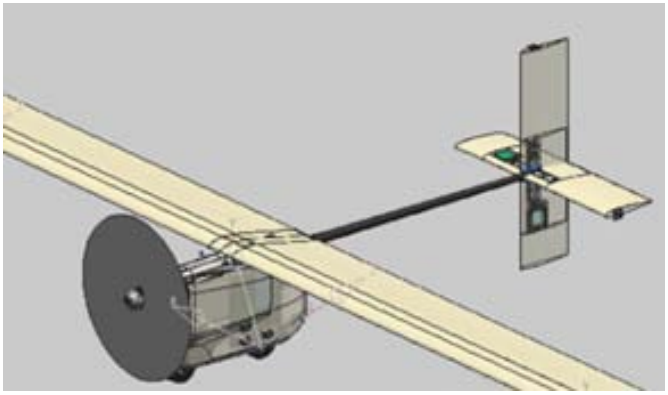

Figure 60. Final Vertical Tail Design

Figure 61. Built Vertical/Horizontal Tail in Vertical Position

4.7 Sensor Selection, Design, and Implementation

Data acquisition is at the heart of the X-HALE program. In order to validate the nonlinear aeroelastic codes listed in chapter 2, X-HALE must be able to provide: 1) Wing strain data to determine the wing position, 2) aircraft orientation and speed, and 3) housekeeping sensor data for the continued operation of the aircraft. Figure 62 shows the proposed sensor layout for the ATV configuration. Table 6 shows the number of sensors and channels required.

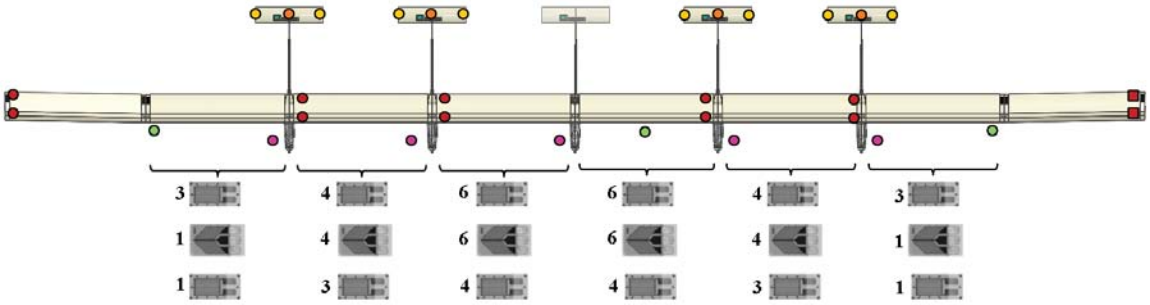

Figure 62. X-HALE Sensor Layout (ATV Configuration)

Table 6. X-HALE Sensor Location and Description

Board/Sensor	Color	Number	Channels	Type
DMM32 I/O PC104 Card		4	64 (Available)	
Bending Strain Gauge		26	26	
Shear Strain Gauge		22	22	Differential
In Plane Strain Gauge		16	16	
Athenia II SBC		4	64 (Available)	
2 Axis Accelerometer		12	24	
1 Axis Accelerometer		8	8	
5 Hole Pitot Probe		3	9	
Tail Potentiometer		4	4	Single Ended
Fairing Housekeeping				
Voltage Divider Circuit		10	10	
Motor RPM		5	5	
Thermocouple*		4	4	

The design team selected two general purpose strain gages manufactured by Vishay: Linear strain gauge 187UW and torsional strain gauge 187UV. Manufacturer data for the strain gauges can be found in Appendix A-17 and A-18. Section 4.3.1 details the installation of the strain gauges. All strain gauges connect to the expansion I/O modules stacked on the Athenia SBC, both of which will be described in section 4.8. A total of 64 strain gauges were placed throughout X-HALE for the ATV configuration. The number of strain gauges was limited to 64 to reduce cost and to maximize the number of A/D ports utilized on the expansion modules. The FTV configuration will only have 12 strain gauges installed to reduce the complexity of the initial testing aircraft.

To measure the accelerations of the wing pods during flight testing, the design team selected a 2 axis accelerometer from Sparkfun. The ADXL 320 is capable of measuring ±5g in two axes and was selected for both its accuracy and its low cost relative to other accelerometers, Appendix A-19. Two one axis accelerometers are placed in each elevon. The design team selected Analog Device's ADXL193 250G accelerometer for use in the tails, Appendix A-22.

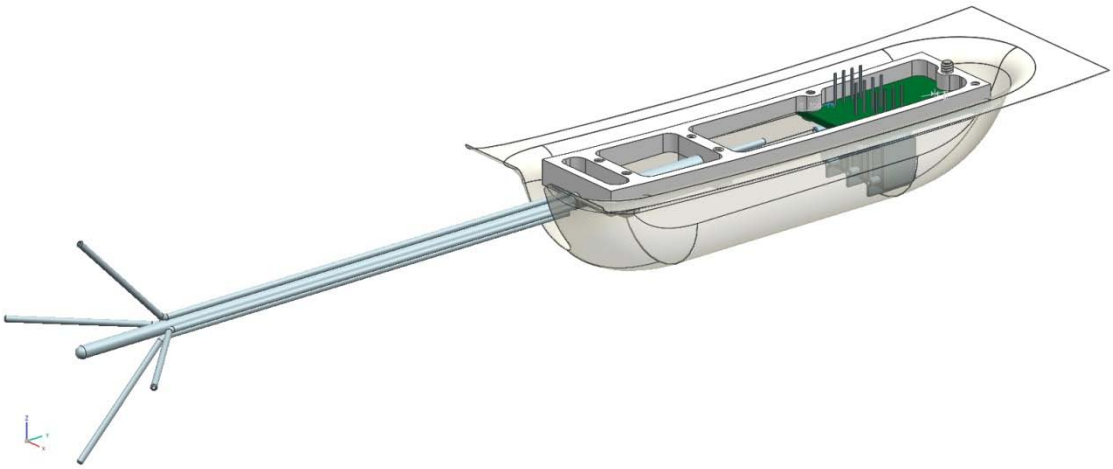

Figure 63. 5 Hole Pitot Probe

Figure 63 above shows the 5 hole pitot probe and the mounting assembly. The 5 hole pitot probe and pressure transducer (Figure 64) provide data that when produced indicates the velocity of the relative wind. The angle of attack and aircraft speed can be deduced from the pitot probe. Mounted directly to the wing tips and near the center fuselage via direct attachment to the wing skin, analog data produced from the probe is routed through the wing to the nearest SBC.

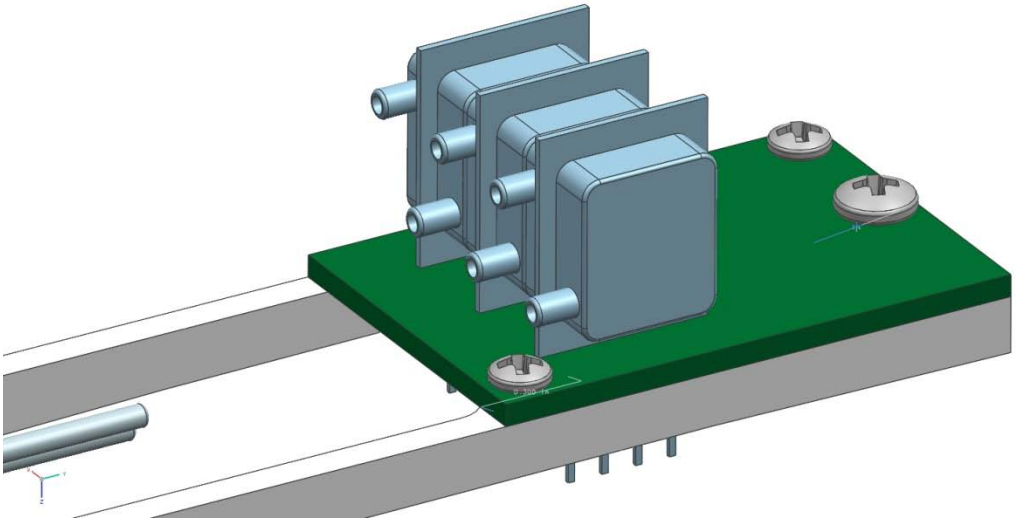

Figure 64. Pressure Transducer

Figure 64 above shows the 3 stacked pressure transducer. The six female ports measure the static pressure of the surrounding air, the total pressure generated by the most forward facing pitot probe, and the remaining four measure the total pressure from each of the angled secondary probes.

Figure 65. The MIDG II GPS/INS

The MIDG II (Figure 65 and Appendix A-8) combines a three axis accelerometer, GPS, and gyroscope into a small self-contained unit. This single unit acts as an inertial navigation system which will provide the aircraft controller data regarding the position and orientation of the aircraft. This data will be used in tandem with the accelerometers and the pitot probes in determining the orientation and velocity of the aircraft. Requiring only 1.2W for operation and measuring only 1.5" by 1.58" by 0.88", the sensor does not constrain the size of the fuselage or demand a significant amount of power from X-HALE's power system. The angular rate sensor's accuracy of 0.05°/sec $\sqrt{\text{Hz}}$ and linear acceleration sensor's accuracy of 150 μg / $\sqrt{\text{Hz}}$ would provide the necessary accuracy for code validation. Due to the cost of the MIDG, it would be unreasonable and unnecessary to place one between each wing module. Also, the NAST code only tracks one body reference frame. Therefore, only one MIDG is installed on the aircraft in the center fairing.

Motor RPM is measured from the ESC. Due to interfacing limitations of the controllers, the data must be downloaded after flight testing. The ESCs also record the commanded inputs, battery voltage, and applied current. This data will be important in determining actual motor power output and will serve as a secondary data storage location if the aircraft looses an engine power during flight testing.

COTS J type thermocouples placed within the fairings provide the controller with the temperature within the fairings. This will aid in the analysis of the FTV and will assist when determining if the airflow through the fairing is sufficient to keep the onboard electronics within temperature tolerances.

4.8 Data Acquisition, Storage, and Transmission

Figure 66. Diamond-MM-32DX-AT I/O Expansion Card (Left) and Athena II SBC

In an attempt to limit cost, power required, and the size of the data processing unit, it was decided that a Diamond Systems Athena II single board computer would be sufficient for data processing and storage, Appendix A-9. Measuring 4.2” by 4.5”, the computer requires a maximum of 8W for operation, well within the power supply limits of the electronics battery. While each Athena SBC includes 16 single-ended analog to digital conversion (ADC) circuits, the computer was supplemented with a Diamond Systems DMM32 I/O PC104 card that adds an additional 16 channels to the computer, Appendix A-10. The housekeeping and scientific sensors throughout the aircraft use 128 channels for the ATV configuration, requiring 4 stacks for data acquisition. Each SBC has a 1GB non-volatile flash card to store collected data. The module in fairing 1 is programmed as the master module and synchronizes the data collection through the use of a pulse per second synchronizing signal. Actual data collection occurs at 1 kHz depending on the sensors

A real-time data link to a field laptop requires a low cost, low power, high range device small enough to fit inside on X-HALE’s fairings. X-HALE uses the 9XStream

900 MHz transmitter/receiver system. This transceiver has a 20 mile line-of-sight range and has an interface data rate up to 57600 bps, Appendix A-24.

4.9 Power and Mass Budget

In addition to the 11.1V 6000mAh battery within each fairing for engine power, each fairing also contains a Thunder Power 11.1V 1320 mAh battery. Table 7 and Table 8 below show the respective power budgets for central and outboard fairings.

Table 7. Central Fairing Power Budget

Users	**Power (W)**	**Duty Factor**	**Energy (Wh)**
MIDG II	1.2	100%	0.9
SSC	0.5	100%	0.38
Radio Modem	1	100%	0.75
Serial Conv	0.02	100%	0.02
Receiver	0.4	100%	0.3
2 Servos	0.46	50%	0.17
Ethernet Hub	5	100%	3.75
30% Contingency	2.574		1.88
Total	3.58		**8.14**
Available			14.65
DOD			**56%**

Table 8. Outboard Fairings Power Budget

Users	**Power (W)**	**Duty Factor**	**Energy (Wh)**
Athena II	10	100%	7.5
Jupiter MM LP	1.5	100%	1.125
PC104	2.05	100%	1.54
2 Servos	0.46	50%	0.09
Total	14.01		**10.25**
Available			14.65
DOD			**70%**

X-HALE's total mass budget originally came to 10.76 kg and a detailed mass budget completed by Senatore can be found in Appendix A-13. The addition of another tail assembly adds 202 g, bringing the total to approximately 11 kg with a 15% contingency.

V. Conclusions and Recommendations

5.1 Summary

Figure 67. Working Model of X-HALE in June 2010

This thesis outlined the development of X-HALE inception to the manufacturing and assembly of flight components. X-HALE was created in order to validate nonlinear aeroelastic codes to include UM/NAST and ASWING. More realistic and accurate nonlinear aeroelastic codes will enable better HALE aircraft designs and more effective controllers that will increase flight safety margins.

X-HALE is a RPA that has two configurations. The FTV (Flight test vehicle) is used for vehicle qualification and data is gathered from the ATV (Aeroelastic Test Vehicle). The FTV lacks most scientific sensors while the ATV includes all sensors. Both configurations can use either 6 or 8 wing modules. With an aspect ratio of either 30 or 40, X-HALE will be able to excite nonlinear aeroelastic responses that will be measured by onboard strain gauges placed throughout the wings. Accelerometers and pitot probes will measure wing orientations and velocities while a GPS/INS records the aircraft's position and records it to onboard computers. Additionally, housekeeping sensors will keep track of engine RPM, fuselage temperatures, and elevon positions for the duration of the flight.

5.2 Lessons Learned from *X-HALE's Construction*

Perhaps the most important lesson from the development of X-HALE was the need to maintain documentation throughout the design and construction process. Besides the benefit to similar programs, program documentation provides future researchers and engineers with the necessary background to rapidly integrate themselves into the program.

Integration of design changes late in the program's construction phase revealed the importance of design adaptability. NAST simulations indicated that X-HALE would become unstable due to a dutch roll like mode during flight and it became necessary to provide lateral stability without affecting the onset of aeroelastic phenomena that X-HALE was built for. The addition of a rotating horizontal to vertical stabilizer proved to be the best solution and shows that without design flexibility, programs may fail due to newfound limits in previously validated designs.

5.3 X-HALE's Next Steps

Currently, the majority of the X-HALE flight components have been manufactured and the design team is proceeding with the integration of those components. Upon the machining of additional joiner blocks, X-HALE will be ready to be assembled for FTV testing. The X-HALE program has effectively completed the physical task of building X-HALE and will require a safety review board (SRB) for permission for flight test once the FTV has been assembled. ATV construction will proceed once the FTV has been flown and the design concept validated. Prior to the flight of the ATV, several tasks will have to be completed. Each wing module will have to be calibrated to determine its strain- displacement relationships. The onboard

computers will have to be ground tested to ensure their functionality. The 5 hole pitot probes will have to be wind tunnel tested and calibrated. An autopilot will have to be created from the data obtained from the FTV in order to effectively excite aeroelastic phenomena.

Once flown, data from the ATV will then be reduced and analyzed and compared with analytical data produced from UM/NAST and the other nonlinear aeroelastic codes. The ATV will most likely be flown several more times as part of the process of iteratively validating and correcting inconsistencies between predicted and actual data.

5.4 Future Additional Documentation

While this document has sought to be as comprehensive as possible, parts of X-HALE's development (both past and future) are missing. Component integration, from joiner block insertion to battery installation, should be added. Wing, accelerometer, and pitot probe calibration data will have to be added when the testing is complete. This document is missing electronic wiring diagrams for the SBC, central custom break out board, and strain gauges. Once the computers have been effectively networked, documentation regarding the process and results will have to be added.

Appendix A. X-HALE Documentation and Component Specifications

Appendix A-1: Shearer's Initial X-HALE Presentation

Appendix A-2: Formax 0/90 E-Glass

Appendix A-3: HexPly F155 E-Glass

Appendix A-4: Rohacell IG/IG-F Foam

Appendix A-5: Properties of IM7/977-3 Graphite

Appendix A-6: Elevon Diagram

Appendix A-7: HS-5125MG Specifications

Appendix A-8: MIDG II Specifications

Appendix A-9: Athena II SBC Specifications

Appendix A-10: Diamond Systems DMM-32DX-AT Specifications

Appendix A-11: Joiner Block Diagram

Appendix A-12: University of Michigan Aerospace Autoclave

Appendix A-13: Initial Mass Budget

Appendix A-14: Fuselage Pod Diagram

Appendix A-15: PJS 1200 Electric Motor Specifications

Appendix A-16: Tail Boom and Fuselage Diagram

Appendix A-17: Vishay 187UW Strain Gauge Specifications

Appendix A-18: Vishay 187UV Strain Gauge Specifications

Appendix A-19: ADXL320 Accelerometer Specifications

Appendix A-20: JR X9303 Transmitter Specifications

Appendix A-21: JR R921 Receiver Specifications

Appendix A-22: ADXL193 Accelerometer Specifications

Appendix A-23: Dave Brown WH25 Lite Wheels Specifications

Appendix A-24: 9XStream (900 MHz) Transceiver Specifications

Bibliography

1. Baker, A. A., Stuart Dutton, and Donald Kelly. *Composite Materials for Aircraft Structures*. Reston, VA: American Institute of Aeronautics and Astronautics, 2004. Print.

2. Bloxham, Andy. "Solar-powered Plane to Fly through Night with Pilot on Board - Telegraph."*Telegraph.co.uk - Telegraph Online, Daily Telegraph and Sunday Telegraph - Telegraph*. Web. 24 Feb. 2011. <http://www.telegraph.co.uk/earth/energy/solarpower/7834381/Solar-powered-plane-to-fly-through-night-with-pilot-on-board.html>.

3. Boyle, Rebecca. "Boeing Wins Bid to Build Vulture, the Solar Spyplane That Stays Aloft for Five Years | Popular Science." *Popular Science | New Technology, Science News, The Future Now*. Web. 24 Feb. 2011. <http://www.popsci.com/technology/article/2010-09/boeing-wins-bid-build-solar-plane-flies-five-years-end>.

4. Davis, Blake. Personal interview. 15 Feb. 2011.

5. Cesnik C. E. S., Senatore P. J., Su W., Atkins M., "X-HALE: A Very Flexible UAV for Nonlinear Aeroelastic Tests." *Cesnik_ET_al_SDM_2010_given*. Ann Arbor, 12 Apr. 2010. PDF

6. Cesnik, C. E. S., Senatore, P. J., Su, W., Atkins, E. M., Shearer, C. M., and Pitcher, N. A., "X-HALE: a Very Flexible UAV for Nonlinear Aeroelastic Tests," Paper No. AIAA-2010-2715, Proceedings of the 51st AIAA/ASME/ASCE/AHS/ASC Structures, Structural Dynamics, and Materials Conference, Orlando, FL, Apr. 12 – 15, 2010

7. Drela, M. , "Integrated Simulation Model for Preliminary Aerodynamic, Structural, and Control-Law Design of Aircraft," Proceedings of the 40th AIAA/ASME/ASCE/AHS/ASC Structures, Structural Dynamics, and Materials Conference and Exhibit, St. Louis, Missouri, April 12–15 1999, pp. 1644–1656, AIAA Paper No. 99-1394.

8. Galitzine, Greg. "U.S. Tests Solar-Powered HALE UAS at Naval Air Warfare Center." Web. 24 Feb. 2011. <http://blog.tmcnet.com/robotics/2009/11/us_tests_solar-powered_hale_uas_at_naval_air_warfare_center.html>.

9. Greene, Nick. "White Knight Launch Aircraft Carries the Spaceship." *Space & Astronomy at About.com*. Web. 24 Feb. 2011. <http://space.about.com/od/privatespaceagencies/p/ss1teamphoto_d.htm>.

10. Heeg, J., Spain, C.V., Florance, J.R., Wisemann C.D., Ivanco, T.G., DeMoss, J.A. & Silva, W.A. “Experimental Results from the Active Aeroelastic Wing Wind Tunnel Test Program. 46th AIAA Structures, Structural Dynamics and Materials Conference 2005. AIAA 2005-2234.

11. Hepperle, Martin. "Basic Design of Flying Wing Models." *Willkommen / Welcome*. 1 Dec. 2002. Web. 12 Feb. 2011. <http://www.mh-erotools.de/airfoils/flywing1.htm>.

12. Hodges, D. H., “Geometrically-exact, intrinsic theory for dynamics of curved and twisted anisotropic beams," *AIAA Journal*, vol. 41, pp. 1131-1137, June 2003.

13. Hodson, H. "Pressure Probes.” 6 Feb. 2011. <http://www-g.eng.cam.ac.uk/whittle/current-research/hph/pressure-probes/pressure-probes-fig-5.gif>

14. Jaworski, Justin. *Aeroelastic Wind Tunnel Testing of Very Flexible High-Aspect-Ratio Wings*. .pdf.

15. Jones, R.I., “The Design Challenge of High Altitude Long Endurance (HALE) Unmanned Aircraft,” *The Aeronautical Journal*, pp. 273-280, 1999.

16. Newman, Daniel. "DARPA - Tactical Technology Office (TTO)." *DARPA – Tactical Technology Office (TTO)*. Web. 05 Jan. 2011. <http://www.darpa.mil/tto/programs/vulture/>.

17. Noll, T. E., Brown, J. M., Perez-Davis, M. E., Ishmael, S.D., Tiffany G.c., and Gaier, M., "Investigation of the Helios Prototype Aircraft Mishap," Tech. rep., NASA, January 2004.

18. Patil, M. J. and Hodges, D. H., “Flight dynamics of highly fexible flying wings," in *CEAS/AIAA/DGLR International Forum on Aeroelasticity and Structural Dynamics, Munich, Germany*, June 28-July 1, 2005.

19. Patil, M. J. and Hodges, D. H., "Nonlinear Aeroelasticity and Flight Dynamics of Aircraft in Subsonic Flow," In Proceedings of the 21st Congress of International Council of the Aeronautical Sciences, Melbourne, Australia, September 1998.

20. Pendleton, E., Voracek D., Flick P., Reichenbach., Griffen K., Paul D., "The X-53: A Summary of the Active Aeroelastic Wing Flight Research Program," Structures, Structural Dynamics, and Materials Conference, Honolulu, Hawaii, Apr. 23-26, 2007.

21. Prentice, E., *Wing_Procedure*. Ann Arbor, 15 Aug 2010. DOC

22. Saberi, H., Khoshlahjeh, M., Ormiston, R. A., and Rutkowski, M.J., “Overview of RCAS and Application to Advanced Rotocraft Problems,” American Helicopter

Society 4th Decennial Specialists' Conference on Aeromechanics, San Francisco, CA, January 2004.

23. Senatore, P., *Wing Layup*. Ann Arbor, 6 Aug 2011. DOCX

24. Senatore, P., *XHALE portfolio*. Ann Arbor, 6 Aug 2011. PDF

25. Senatore, P., Cesnik, C. E. S., Su, W., *XHALE Overview.ppt*. Ann Arbor, 2 Oct 2009. PPTX

26. Shearer, Chris. *Building a Flying Scaled High Altitude HALE Aircraft*. Ann Arbor, 27 Aug 2008. PPT

27. Shearer, C. M. and Cesnik, C. E., "Nonlinear Flight Dynamics of Very Flexible Aircraft," San Fransisco, CA, August 15 - 18 2005, AIAA Paper No. 2005-5805, also J. Aircraft, 2007.

28. Shearer, C. M. and C. E. S. Cesnik. "Modified Generalized Alpha Method for Integrating Governing Equations of Very Flexible Aircraft." AIAA-2006-1747, *47th AIAA / ASME / ASCE / AHS / ASC Structures, Structural Dynamics, and Materials Conference*, Newport, RI, May 1-4, 2006.

29. Shearer, C. M. and C. E. S. Cesnik. *X-HALE_TestPlan_v19_19Oct2010*. Ann Arbor, 19 Oct. 2010. DOC.

30. Shearer, Chris. Personal interview. 4 Feb. 2011.

31. Shirk, M. H., Hertz, T. J., and Weisshaar, T. A., "Aeroelastic Tailoring - Theory, Practice, and Promise," Journal of Aircraft, Vol. 23, No. 1, Jan. 1986, pp. 6 - 18.

32. Sotoudeh, Z., Chang, C.-S., and Hodges, D. H., "Validation Studies for Nonlinear Aeroelastic Trim and Stability of HALE aircraft," *CEAS/AIAA/DGLR International Forum on Aeroelasticity and Structural Dynamics, Seattle, Washington* June 22–24 2009.

33. Su, W., and Cesnik, C. E. S., "Nonlinear Aeroelastic Simulations of a Flapping Wing Micro Air Vehicle Using Two Unsteady Aerodynamic Formulations," AIAA-2010-2887, *51st AIAA/ASME/ASCE/AHS/ASC Structures, Structural Dynamics, and Materials Conference,* Orlando, FL, 12 - 15 April, 2010.

34. Su, W., and Cesnik, C. E. S., "Nonlinear Aeroelasticity of a Very Flexible Blended-Wing-Body Aircraft," *Journal of Aircraft*, Vol. 47, No. 5, 2010, pp. 1539-1553, doi: 10.2514/1.47317

35. Tang, D. and Dowell, E.H., *"Experimental and Theoretical Study on Aeroelastic Response of High-Aspect-Ratio Wings"*, AIAA Journal, Vol. 39, No. 8, August 2001, pp. 1430-1441.

36. Tilmann, C.P. Flick, P.M, Martin, C.A., and Love M.H., "High-Altitude Long Endurance Technologies for Sensorcraft," RTO AVT Symposium on "Novel Vehicle Concepts and Emerging Vehicle Technologies," Brussles, Belgium, April 7-10 2003, MP-104-P-26-1.

37. Utc, 15-Nov-2006 08:19. "$113M to Raytheon to Support U-2 Spy Planes." *Defense Industry Daily - Military Purchasing News for Defense Procurement Managers and Contractors*. Web. 24 Feb. 2011. <http://www.defenseindustrydaily.com/113m-to-raytheon-to-support-u2-spy-planes-02799/>.

38. Van Schoor, M.C. and von Flotow, A.H., "Aeroelastic Characteristics of a Highly Flexible Aircraft," *Journal of Aircraft*, Vol. 27, No. 10, pp. 901–908, 1990.

39. aanon., "Unmanned Aircraft Systems Roadmap 2005-2030," Tech. rep., Office of the Secretary of Defense, Department of Defense, 4 August 2005.

REPORT DOCUMENTATION PAGE

Form Approved
OMB No. 074-0188

1. REPORT DATE *(DD-MM-YYYY)*	**2. REPORT TYPE**	**3. DATES COVERED** *(From – To)*
28 March 2011	Master's Thesis	March 2010 – March 2011

4. TITLE AND SUBTITLE

X-HALE: The Development of a Research Platform for the Validation of Nonlinear Aeroelastic Codes

5a. CONTRACT NUMBER

5b. GRANT NUMBER

5c. PROGRAM ELEMENT NUMBER

6. AUTHOR(S)

Public, Alexander A Kaszynski, 2nd Lieutenant, USAF

5d. PROJECT NUMBER

5e. TASK NUMBER

5f. WORK UNIT NUMBER

7. PERFORMING ORGANIZATION NAMES(S) AND ADDRESS(S)
Air Force Institute of Technology
Graduate School of Engineering and Management (AFIT/EN)
2950 Hobson Way, Building 640
WPAFB OH 45433-8865

8. PERFORMING ORGANIZATION REPORT NUMBER

AFIT/GAE/ENX/11-M15

9. SPONSORING/MONITORING AGENCY NAME(S) AND ADDRESS(ES)

Intentionally left blank

10. SPONSOR/MONITOR'S ACRONYM(S)

11. SPONSOR/MONITOR'S REPORT NUMBER(S)

12. DISTRIBUTION/AVAILABILITY STATEMENT

APPROVED FOR PUBLIC RELEASE; DISTRIBUTION UNLIMITED.

13. SUPPLEMENTARY NOTES

14. ABSTRACT In conjunction with the Air Force Institute of Technology (AFIT) and the Air Force Research Laboratory (AFRL), the University of Michigan has designed and is currently building a remotely piloted aircraft (RPA) experimental high altitude long endurance (X-HALE) aircraft to collect non-linear aeroelastic data to validate HALE aircraft design codes developed by academia, industry, and the federal government. While X-HALE is representative of HALE aircraft, the manufacturing and evaluation techniques are applicable to larger full size HALE aircraft such as the concepts being developed under Defense Advanced Research Projects Agency's (DARPA's) Vulture program. This paper documents the development of the X-HALE model to date including a history of the programmatic decisions, basic model configuration, geometric considerations, sensor and system architecture, and manufacturing challenges. Lessons learned from the prototyping include the evolutionary growth of X-HALE's joiner blocks and the manufacturing process of the composite wings. Furthermore, late in the design process, a series of aeroelastic simulations using the Nonlinear Aeroelastic Simulation Toolbox (NAST) developed at the University of Michigan demonstrated the need for a rotating vertical/horizontal stabilizer to aid in the recovery of the vehicle from unstable nonlinear coupled lateral dynamic "dutch roll like" motion. The documentation and development of X-HALE is critical to the programmatic goal of providing a complete nonlinear aeroelastic data set for the validation of nonlinear aeroelastic analytical tools for government, industry and academia.

15. SUBJECT TERMS
Aircraft, high altitude, long endurance

16. SECURITY CLASSIFICATION OF:			**17. LIMITATION OF ABSTRACT**	**18. NUMBER OF PAGES**	**19a. NAME OF RESPONSIBLE PERSON**
a. REPORT	**b. ABSTRACT**	**c. THIS PAGE**			Christopher Shearer, Lt Col, USAF
U	**U**	**U**	**UU**	112	**19b. TELEPHONE NUMBER** *(Include area code)* (937) 255-3636, ext 4587 (christopher.shearer@afit.edu)

Standard Form 298 (Rev. 8-98)
Prescribed by ANSI Std. Z39-18